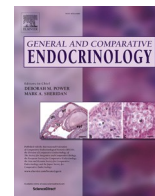Contents lists available at ScienceDirect

General and Comparative Endocrinology

journal homepage: www.elsevier.com/locate/ygcen

Research paper

Leptin receptor-deficient (knockout) zebrafish: Effects on nutrient acquisition

Gianmarco Del Vecchio [a,b,1], Koji Murashita [b,c,1], Tiziano Verri [a], Ana S. Gomes [b], Ivar Rønnestad [b,*]

[a] Department of Biological and Environmental Sciences and Technologies, University of Salento, Via Provinciale Lecce-Monteroni, I-73100 Lecce, Italy
[b] Department of Biological Sciences, University of Bergen, PO Box 7803, NO-5020 Bergen, Norway
[c] Aquaculture Research Department, Fisheries Technology Institute, Fisheries Research and Education Agency, 224-1 Hiruda, Tamaki, Watarai, Mie 519-0423, Japan

ABSTRACT

In mammals, knockout of *LEPR* results in a hyperphagic, morbid obese, and diabetic phenotype, which supports that leptin plays an important role in the control of appetite and energy metabolism, and that its receptor, *LEPR*, mediates these effects. To date, little is known about the role(s) of *lepr* in teleost physiology. We investigated a zebrafish (*Danio rerio*) homozygous *lepr* knockout (*lepr*$^{-/-}$) line generated by CRISPR/Cas9 in comparison to its *wt* counterpart with respect to nutrient acquisition, energy allocation, and metabolism. The metabolic characterization included oxygen consumption rate and morphometric parameters (yolk sac area, standard length, wet weight, and condition factor) as proxies for use and allocation of energy in developing (embryos, larvae, and juveniles) zebrafish and showed no particular differences between the two lines, in agreement with previous studies. One exception was found in oxygen consumption at 72 hpf, when zebrafish switch from embryonic to early larval stages and food-seeking behavior could be observed. In this case, the metabolic rate was significantly lower in *lepr*$^{-/-}$ than in *wt*. Both phenotypes showed similar responses, with respect to metabolic rate, to acute alterations (22 and 34 °C) in water temperature (measured in terms of Q_{10} and activation energy) compared to the standard (28 °C) rearing conditions. To assess *lepr* involvement in signaling the processing and handling of incoming nutrients when an exogenous meal is digested and absorbed, we conducted an *in vivo* analysis in *lepr*$^{-/-}$ and *wt* early (8 days post-fertilization) zebrafish larvae. The larvae were administered a bolus of protein hydrolysate (0%, 1%, 5%, and 15% lactalbumin) directly into the digestive tract lumen, and changes in the mRNA expression profile before and after (1 and 3 h) administration were quantified. The analysis showed transcriptional differences in the expressions of genes involved in the control of appetite and energy metabolism (*cart*, *npy*, *agrp*, and *mc4r*), sensing (*casr*, *t1r1*, *t1r3*, *t1r2-1*, *t1r2-2*, *pept1a*, and *pept1b*), and digestion (*cck*, *pyy*, *try*, *ct*, and *amy*), with more pronounced effects observed in the orexigenic than in the anorexigenic pathways, suggesting a role of *lepr* in their regulations. Differences in the mRNA levels of these genes in *lepr*$^{-/-}$ *vs. wt* larvae were also observed. Altogether, our analyses suggest an influence of *lepr* on physiological processes involved in nutrient acquisition, mainly control of food intake and digestion, during early development, whereas metabolism, energy allocation, and growth seem to be only slightly influenced.

1. Introduction

Mammalian leptin functions as a circulating signal for triglyceride (energy) stores in both white and brown adipose tissue, and plasma leptin concentrations are positively correlated with triglyceride stores (Maffei et al., 1995; Rosenbaum et al., 1996). Within the central nervous system (CNS), leptin receptor isoforms (LEPRs) (Chen et al., 1996)

control most of the effects of circulating leptin on feeding behavior (Banks et al., 2004; Fruhbeck, 2006; Pelleymounter et al., 1995), substrate (lipid and carbohydrate) utilization in peripheral organs (Havel, 2004), puberty (Elias and Purohit, 2013), and reproductive biology (Moschos et al., 2002; Zieba et al., 2005). LEPRs are located in the hypothalamus, that comprises neurons producing both orexigenic (stimulating) and anorexigenic (inhibiting) neuropeptides, all of which

* Corresponding author.
  E-mail address: Ivar.Ronnestad@uib.no (I. Rønnestad).
[1] These authors contributed equally to this study.

involved in appetite control. Leptin acts as a satiety factor by blocking the synthesis and secretion of orexigenic neuropeptides (neuropeptide Y [NPY] and agouti-related protein [AgRP]) (Erickson et al., 1996; Wilson et al., 1999) and by promoting the secretion of anorexigenic neuro-peptides (pro-opiomelanocortin [POMC] and cocaine- and amphetamine-regulated transcript [CART]) (Boston et al., 1997; Elias et al., 1998; Kristensen et al., 1998). In addition to adipose tissues, leptin is also produced in the gut, where it specifically affects many digestive functions, such as the upregulation of the peptide transporter SoLute Carrier family 15 member 1 (*SLC15A1*, aka PEPT1) involved in the absorption of dietary di- and tripeptides (Yarandi et al., 2011). In mammals, *LEPR*-deficient mice results in a hyperphagic and obese phenotype with diabetes (Hummel et al., 1966), which supports the notion that leptin plays an important role in the control of appetite and energy metabolism, and that LEPR mediates leptin effects on energy homeostasis (Zhang and Chua, 2018).

In teleosts, the role of leptin is unclear. This hormone was first identified by Kurokawa et al. (2005) in pufferfish (*Takifugu rupribes*) and later in other species, such as common carp (*Cyprinus carpio*) (Huising et al., 2006), zebrafish (*Danio rerio*) (Gorissen et al., 2009), medaka (*Oryzias latipes*) (Kurokawa and Murashita, 2009), and Atlantic salmon (*Salmo salar*) (Rønnestad et al., 2010). Unlike in mammals, the liver appears to be the main source of leptin synthesis in teleosts; however, the hormone is also found in other tissues, including the brain, adipose tissue, intestine, and gonads (Kurokawa et al., 2005; Kurokawa and Murashita, 2009; Liu et al., 2010; Rønnestad et al., 2010), with large variability depending on the species examined. Since adipose tissue is not the major source of leptin in fish, the correlation with lipid levels is currently not clear as it is in mammals. Moreover, due to whole-genome duplication events, teleosts may potentially harbor two to four *lep* and *lepr* paralogs depending on family affiliation. For example, zebrafish (Cyprinidae) contain two leptin paralogs, *lepa* and *lepb* (Gorissen et al., 2009; Gorissen and Flik, 2014; Londraville et al., 2014), with *lepa* mainly expressed in the liver (Kurokawa et al., 2005; Kurokawa and Murashita, 2009; Liu et al., 2010; Rønnestad et al., 2010), and *lepb* mostly confined to the CNS (Angotzi et al., 2013; Ohga et al., 2015; Yuan et al., 2016) or ovaries (Gorissen et al., 2009). These findings suggest different and unique functions of leptin paralogs in fish compared with those in mammals.

Leptin exerts its effect through the leptin receptor and modulates feeding behavior in fish, although these findings were reported to be inconclusive (Zhang and Chua, 2018). In goldfish (*Carassius auratus*), for example, leptin (both recombinant leptin-A1 and -A2; intraperitoneal administration) inhibits feeding behavior and reduces total feed con-sumption (Yan et al., 2016). In addition, decreased mRNA levels of orexigenic *orexin*, *npy*, and *agrp* and increased mRNA levels of anorexi-genic *pomc* and *cart* have been observed (Yan et al., 2016). In medaka, *lepr* exerts a powerful influence on the control of food intake (Chisada et al., 2014). In fact, the mutant medaka (homozygous *lepr* gene muta-tion) exhibits hyperphagia in post-juvenile and adult stages, leading to a higher growth rate than that in the wild type (*wt*). Although final adult body sizes were not significantly different, the *lepr⁻/⁻* knockout type showed large deposits of visceral fat, unlike the *wt* (Chisada et al., 2014). Moreover, the mutant medaka showed consistently upregulated mRNA levels of the orexigenic *npya* and *agrp* and suppressed levels of the anorexigenic *pomc* genes (Chisada et al., 2014). On the other hand, available data on zebrafish show that adult individuals lacking a func-tional *lepr* (*lepr⁻/⁻* knockout type) do not exhibit hyperphagia or increased adiposity and do have normal fertility (Michel et al., 2016), but, increased levels of insulin expression and modifications in glucose homeostasis have been reported (Michel et al., 2016). Leptin has pre-viously been suggested to play a role in energy expenditure during endogenous feeding in zebrafish, a period when all the necessary nu-trients for development, growth, and energy metabolism are present and acquired from the yolk sac (Dalman et al., 2013; Liu et al., 2012).

In synthesis, with respect to energy acquisition and allocation, it appears that some species of *lepr*-deficient fish exhibit close-to-normal physiology (Fei et al., 2017; Michel et al., 2016), while others exhibit altered physiology (Chisada et al., 2014), compared with those in *wt* fish. The reported contradictory data are indicative of the independent evolution of leptin genes and species-specific responses, with the consequence of the different metabolic adaptations observed (Rønnestad et al., 2017). Moreover, it is likely that leptin plays a major role in the regulation of glucose homeostasis, and this appears to be a conserved function across vertebrates, whereas leptin, as a lipostatic factor, is likely to have acquired a new function during mammalian evolution (Michel et al., 2016).

Using a leptin receptor knockout (*lepr⁻/⁻*) line, we aimed to describe the role of *lepr* in energy acquisition, energy metabolism, and energy allocation during zebrafish development, specifically in the embryonic-to-early larval stage, when all the nutrients are directly supplied from the yolk, and in the immediately following larval-to-juvenile stage, when the growing fish ingest food that is digested and assimilated by the gut. We analyzed oxygen consumption and morphometric parameters (yolk utilization rate and growth) as they provide good estimates of the use and allocation of energy resources during development. Since fish are ectotherms, we also explored whether *lepr*-mediated signaling is involved in adjusting the metabolic sensitivity and acute response of energy consumption as a function of water temperature. Moreover, since leptin may be involved in signaling the metabolic allocation of incoming nutrients when a meal is digested and absorbed, we evaluated differ-ences in the dynamic response of selected key genes involved in appetite control, intestinal nutrient sensing, digestion, and absorption after the administration of increasing concentrations of protein (lactalbumin) hydrolysate into the digestive tracts of *lepr⁻/⁻* and *wt* feeding larvae.

2. Materials and methods

2.1. Fish

Fish (AB line) were kept in the Zebrafish Facility at the Department of Biological Sciences of the University of Bergen (Bergen, Norway). Adult fish were maintained under standard rearing conditions (26–28 °C under a 14/10 h day/night light cycle) and fed a commercial diet (ZEBRAFEED; Sparos, Olhão, Portugal) and *Artemia* nauplii to satiation twice a day. Embryos and larvae were maintained at 28 °C and raised in E3 buffer (5 mM NaCl, 0.17 mM KCl, and 0.33 mM $MgSO_4$) until 14 days post-fertilization (dpf). Procedures for generating the *lepr⁻/⁻* fish line, euthanasia of adult fish, and experiments on larvae and juveniles were approved by the Norwegian National Animal Research Authority at Mattilsynet (FOTS ID8750).

2.2. Generation of the lepr⁻/⁻ zebrafish line

2.2.1. Single-guide RNA and Cas9 mRNA preparation

Lepr gene-specific single-guide RNA (sgRNA) and Cas9 mRNA were synthesized based on the method of Ansai and Kinoshita (2014). The 20-base-pair (bp) region 5′-CAGTTCTGACATCAGATACA-3′ with the PAM site (CGG) on the eighth exon of *lepr* was selected as the target site. An appropriately designed pair of oligonucleotides (final concentration: 10 μM each) was annealed in 10 μL of annealing buffer (pH 8.0, 40 mM Tris-HCl, 20 mM $MgCl_2$, and 50 mM NaCl) by heating to 95 °C for 2 min. The mixture was then cooled slowly to 25 °C in 1 h. The pDR274 vector (Addgene Plasmid 42250; Addgene, Watertown, MA, USA) was digested with BsaI-HF (New England Biolabs, Ipswich, MA, USA), and annealed oligonucleotides were ligated into the digested vector. The ligated sgRNA vector was digested with DraI, and sgRNA was synthesized using the AmpliScribe T7-Flash Transcription Kit (Epicentre Biotechnologies, Madison, WI, USA). For Cas9 mRNA synthesis, the pCS2 + hSpCas9 vector (Addgene Plasmid 51815) was linearized by NotI digestion, and capped RNA was synthesized using the mMESSAGE mMACHINE SP6 Transcription Kit (Thermo Fisher Scientific, Waltham, MA, USA). The

synthesized sgRNA and Cas9 mRNA were purified using the RNeasy Mini Kit (Qiagen, Hilden, Germany).

2.2.2. CRISPR and line generation

Approximately 1.5–2.5 nL of synthesized sgRNA (50 ng/μL) and Cas9 mRNA (100 ng/μL) mixture were injected into fertilized eggs, prior to first cleavage. At that time, the remainder of the sibling eggs were kept and bred as the control *wt* AB line. The sgRNA/Cas9 injected F0 fish were mated with *wt* AB line fish to obtain the F1 generation. The stable genomic mutations of F1 were sequenced and screened (see below Section 2.2.3). F2 generation was established by outcrossing two F1 individuals containing the same 16-bp insertion in exon 8 with *wt* fish, and the progenies were combined. The population expanded from F2 by sibling mating.

2.2.3. Genotype screening

The sgRNA activity (induction rate of somatic mutation) in 2 dpf F0 embryos ($n = 16$), its germ line transmission rate in 2 dpf F1 embryos (offspring of F0 founder and *wt*, $n = 24$), and induced mutation in adult tail fin clips of F0, F1, and F2 were analyzed by nested-PCR-based high-resolution melting (HRM) assay (Kuroyanagi et al., 2013). Genomic DNA was extracted using proteinase K (10 μg/50 μL reaction volume) with lysis buffer (pH 8.0, 10 mM Tris-HCl, 0.1 mM EDTA, and 0.2% Triton X-100) at 50 °C for 1 h, followed by inactivation of proteinase K at 99 °C for 15 min. The 1st-PCR was performed using the primer pair HRM F1 and HRM R1 (see Supplementary Table 1). The 1st-PCR product was diluted in water (150-fold), and 2 μL was used as a template for the second step of the PCR reaction in 10 μL volume. The 2nd-PCR and HRM analyses were performed using a CFX96 Touch System (Bio-Rad Laboratories, Hercules, CA, USA), with SsoFast EvaGreen Supermix (Bio-Rad Laboratories). The primer pair HRM F2 and HRM R2 (Supplementary Table 1) were used for the 2nd-PCR/HRM assay. The HRM 1st-PCR products were also sequenced for the line generation. To confirm if the induced genomic mutation was actually transcribed in the mutant, partial cDNA sequence of *lepr* was obtained from single PCR products using the primer pair lepr F and lepr R which are designed over the different exons (Supplementary Table 1). The cDNA was synthesized from the F3 mutant larvae as described in Section 2.3.3. The PCR products were resolved in an agarose gel electrophoresis, purified using a QIAquick Gel Extraction Kit (Qiagen, Hilden, Germany) and then cloned into a pCR4-TOPO vector (Thermo Fisher Scientific). The inserts were sequenced at the University of Bergen Sequencing Facility (Bergen, Norway), using BigDye v3.1 (Thermo Fisher Scientific) according to the facility protocol.

2.3. Experimental design

For metabolic characterization, $lepr^{-/-}$ and *wt* fish lines were analyzed at various developmental stages. After fertilization, zebrafish embryos and early larvae were analyzed every 24 h ($n = 60$ at each developmental stage and temperature) until 120 h post-fertilization (hpf), when the switch from endogenous to exogenous feeding occurs. Next, zebrafish larvae and juveniles were characterized every seven days (larvae, $n = 48–60$ at each developmental stage; juveniles, $n = 15$ at each developmental stage) until 40 dpf.

To evaluate the effects of food on the early expression of a set of gut and brain genes involved in appetite control, digestion, and nutrient acquisition, 8 dpf zebrafish larvae ($n = 8$) were selectively administered with a bolus of a protein-containing solution as described below (for details see *2.3.3. Tube-feeding test* paragraph).

2.3.1. Respirometry

Oxygen uptake was analyzed by closed respirometry (FireStingO$_2$, Pyro Science, Aachen, Germany). Oxygen concentrations were analyzed in incubation vials using fiber-optic oxygen sensors connected to one of four channels of an optical oxygen meter. The oxygen meter recorded

the signals emitted by the integrated sensor stripes in the chamber walls using REDFLASH technology. The chambers were connected to the fiber cables using adapter rings and were placed in a water bath (Dyneo DD-601F; Julabo, Seelbach, Germany) set at a predetermined temperature (22, 28, or 34 °C, according to the analysis). The recordings were displayed using the Pro Oxygen Logger software (Pyro Science) during respirometry, which had variable duration, depending on fish age and metabolism. The analyses ended before oxygen concentration reached 75–80% of the total, and different assays were performed at different time intervals during the incubation, with 2 min per measurement (≈ 1 measurement per s) in each assay.

Measurements were performed at six developmental time-points (3, 24, 48, 72, 96, and 120 hpf), across three temperatures: 28 °C, the zebrafish standard maintenance temperature, and at 22 and 34 °C, two conditions taken as lower and higher values than the standard, respectively. At each time-point and temperature, six chambers were used, each with 10 individuals in a single 5 mL glass chamber calibrated volume and two blanks.

The temperature coefficient, Q_{10}, for the oxygen uptake was calculated as a response to acute changes in water temperature according to the following equation:

$$Q_{10} = \frac{M_2^{\frac{10}{T_2 - T_1}}}{M_1}$$

where M is the oxygen uptake (nmol/h/individual) at two different temperatures, T (°C), with $T_2 > T_1$.

Moreover, we calculated activation energy (E_a) as an index of temperature dependence using the equation (Arrhenius equation):

$$\ln\left(\frac{M_2}{M_1}\right) = -\frac{E_a}{R}\left(\frac{T_1 - T_2}{T_1 T_2}\right)$$

where M is the oxygen uptake (nmol/h/individual) at two different temperatures, T (°K), and R is the universal gas constant, with $T_2 > T_1$.

After the onset of first feeding, measurements were performed only at standard rearing temperature, that is, 28 °C, using the same respirometer set-up as for embryos and early larvae, and recorded at 6 time-points (5, 12, 19, 26, 33, and 40 dpf). Since larvae and juveniles were incrementally large, we reduced the number of animals per vial: $n = 8–10$ in a single 5 mL glass chamber on 5, 12, and 19 dpf; and $n = 1$ per chamber (5 mL) on 26, 33, and 40 dpf. For the same reason, for larvae (5, 12, and 19 dpf), oxygen uptake was calculated as nmol/h/individual, whereas for juveniles (26, 33, and 40 dpf), oxygen uptake was calculated as nmol/h/mg. Six vials with incubating larvae and two blank vials were used for each sampling point at 5, 12, and 19 dpf, whereas 15 vials with individual larvae and five blanks were used for each sampling point at 26, 33, and 40 dpf.

2.3.2. Yolk utilization rate and growth

Yolk consumption was assessed as a reduction of the yolk-sac area with time during the embryonic and early larval stages. Growth was calculated for larvae and juveniles using standard length (*SL*), wet weight (*WW*), and Fulton's condition factor (*K*), and these measurements were recorded starting from 5 dpf, that is, after the intestine became functional and exogenous feeding commenced. For the yolk-sac area (embryos and early larvae) and *SL* (larvae and juveniles), 10–15 individuals per time-point were anesthetized using Tricaine solution (16 μg/mL). An Olympus SZ 11 microscope (Olympus, Tokyo, Japan) equipped with a Moticam 1080 (MoticEurope, Barcelona, Spain) camera and imaging software Motic Image Plus 3.0 were used to analyze stages up to 12 dpf. Additionally, a Leica M420 (AssetRelay, Symbol Test System Inc., Gatineau, Quebec, Canada) equipped with an Infinity 3 Lumenera (Ottawa, Ontario, Canada) microscope camera and the microscope imaging software Image-Pro® Premium (Media Cybernetics Inc., Rockville, MD, USA) were used to analyze 19, 26, 33, and 40 dpf fish. All pictures were processed with ImageJ v.1.51j8 software (Wayne

Rasband, National Institutes of Health, Bethesda, MD, USA). Representative pictures for the calculation of the yolksac area and *SL* are shown in Supplementary Fig. 1A and 1B, respectively.

For *WW* measurements, 15 larvae and juveniles, 26, 33, and 40 dpf, were anesthetized using Tricaine solution (16 µg/mL) and gently placed into a paper to remove excess water. Weight was then recorded.

The condition factor, *K,* was calculated for larvae and juveniles at 26, 33, and 40 dpf, as the relationship between *WW* and *SL*, according to the following equation:

$$K = 100 * WW/SL^3$$

with *WW* expressed in g and *SL* expressed in cm.

2.3.3. Tube-feeding test and quantitative real time PCR (qPCR) assays

To evaluate the effect of protein administration on larvae, a tube-feeding test was conducted based on the method of Rønnestad et al. (2001). *lepr*$^{-/-}$ and *wt* larvae (8 dpf; 18 h fasted) were fed a single bolus (32 nL) of lactalbumin hydrolysate at different concentrations (0%, 1%, 5%, and 15% w/w) dissolved in 0.9% NaCl (containing 0.2% bromophenol blue as a visual indicator) directly into the digestive tract ($n = 8$). The larvae were sampled and stored in RNAlater (Thermo Fisher Scientific) at the following time-points: before (0), 1, and 3 h after the administration of the protein hydrolysate. The head and trunk of larvae were divided after RNAlater storage, and the following genes were analyzed: *npy, agrp, mc4r, cart3, pept1a, pept1b, casr, t1r1, t1r2-1, t1r2-2, t1r3, ccka, cckb, pyya, pyyb, try, cy,* and *amy*.

mRNA expression levels were analyzed as follows: total RNA was isolated from the samples using Sepasol®-RNAISuper G (Nakalai Tesque, Osaka, Japan), and the purity of the isolated RNA was verified by measuring the optical density (*OD*) absorption ratio at 260 and 280 nm (OD_{260}/OD_{280}), using an e-spect spectrophotometer (Malcom, Tokyo, Japan). Samples with $OD_{260}/OD_{280} > 1.8$ were used for subsequent cDNA synthesis. Genomic DNA elimination and reverse transcription were performed using a Verso cDNA Synthesis Kit (Thermo Fisher Scientific). Subsequently, the mRNA levels of target genes were analyzed using a LightCycler®96 System (Roche, Basel, Switzerland) with THUNDERBIRD SYBR qPCR Mix (Toyobo, Osaka, Japan), according to the manufacturer's instructions; 0.3 µM of each primer at a final concentration with 7.5 µL of premix in a total of 15 µL reaction volume. The PCR parameters consisted of 95 °C for 60 s (initial denaturation), followed by 40 cycles at 95 °C for 10 s (denaturation) and 60 °C for 30 s (annealing and extension). The PCR efficiency of the reaction was determined using the PCR product standard curve. The primer pairs used in each assay were designed based on the nucleotide sequences deposited in the NCBI or Ensembl databases (Supplementary Table 1). Melting temperature analyses revealed a single melting peak. The amount of mRNA was calculated as copies per nanogram of total RNA.

2.4. Statistical analysis

Oxygen uptake, yolk utilization rate, growth (*SL, WW*, and *K*), and transcriptional expression analyses were tested for normality to ensure normal distribution (outliers were removed). All data are expressed as mean ± standard error (SE). Details on the statistical analyses performed in each experimental data set are given in the legends to the figures.

All tests and graphics were performed using GraphPad Prism 8 (GraphPad Software, La Jolla, CA, USA).

3. Results

3.1. Generation of the lepr$^{-/-}$ zebrafish line

A targeted mutation was introduced using CRISPR/Cas9 into the eighth exon region of the zebrafish *lepr* gene (Fig. 1A). As expected, a variety of mosaic mutations were detected in the F0 generation, and the
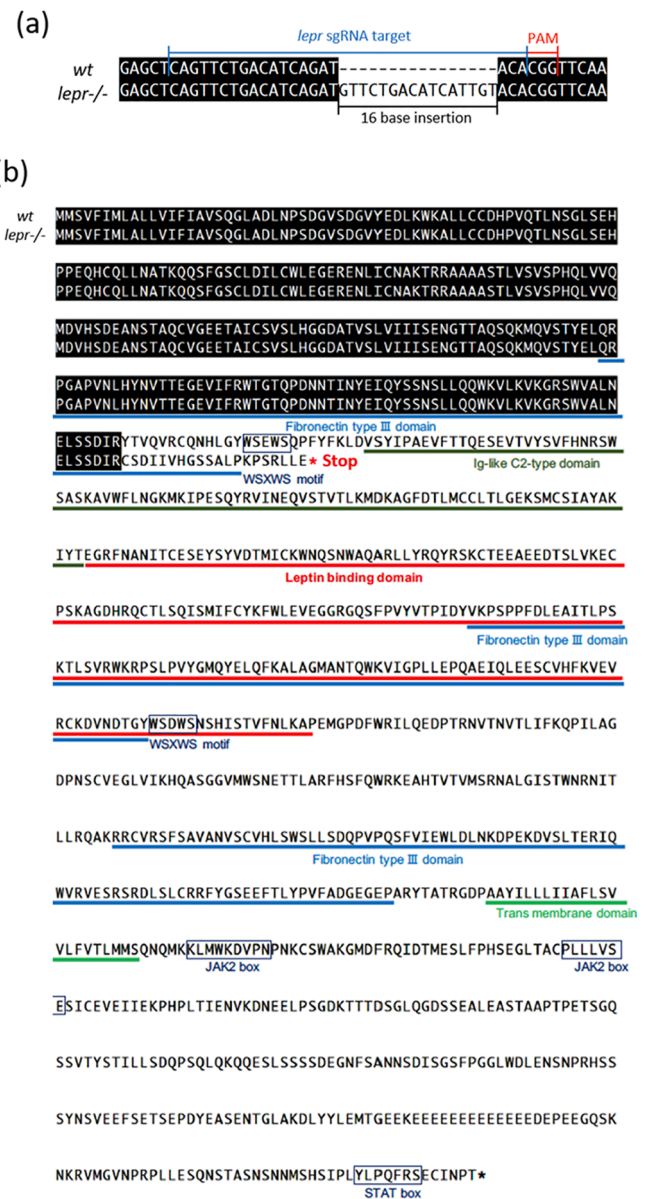

Fig. 1. Generation of the *lepr* knockout (*lepr*$^{-/-}$) line. (A) CRISPR/Cas9 was used to target a 20-base pair (bp) region of exon eight in the zebrafish *lepr* gene. (B) The frameshifted *lepr* mutant yielded a truncated protein, due to an additional region of altered translation in which a stop codon was generated upstream the functionally important Ig-like C2-type domain of the *lepr* gene. The domains were estimated from human LEPR (GenBank Acc. No. AAA93015).

mutation induction rate was 94%. The germline transmission rate of mutations in the F1 generation embryos was 91%. In F1, a stable 16-bp insertion occurring at residue 248, resulting in a frameshift and premature stop codon after 20 nonsense amino acids, was identified for expanding the line (Fig. 1B). The induced mutation of the 16-bp insertion was also confirmed in the cDNA sequence of *lepr*.

3.2. Metabolic characterization

3.2.1. Analysis of oxygen uptake in embryos/early larvae

Oxygen uptake was measured during the embryonic and early larval stages every 24 h, from 3 hpf (t_0) until 120 hpf (the endogenous feeding period). Oxygen uptake increased steadily during development, with comparable trends in both *lepr*$^{-/-}$ and *wt* fish (Fig. 2) at each temperature investigated (i.e., 22, 28, and 34 °C). Overall, the three curves did
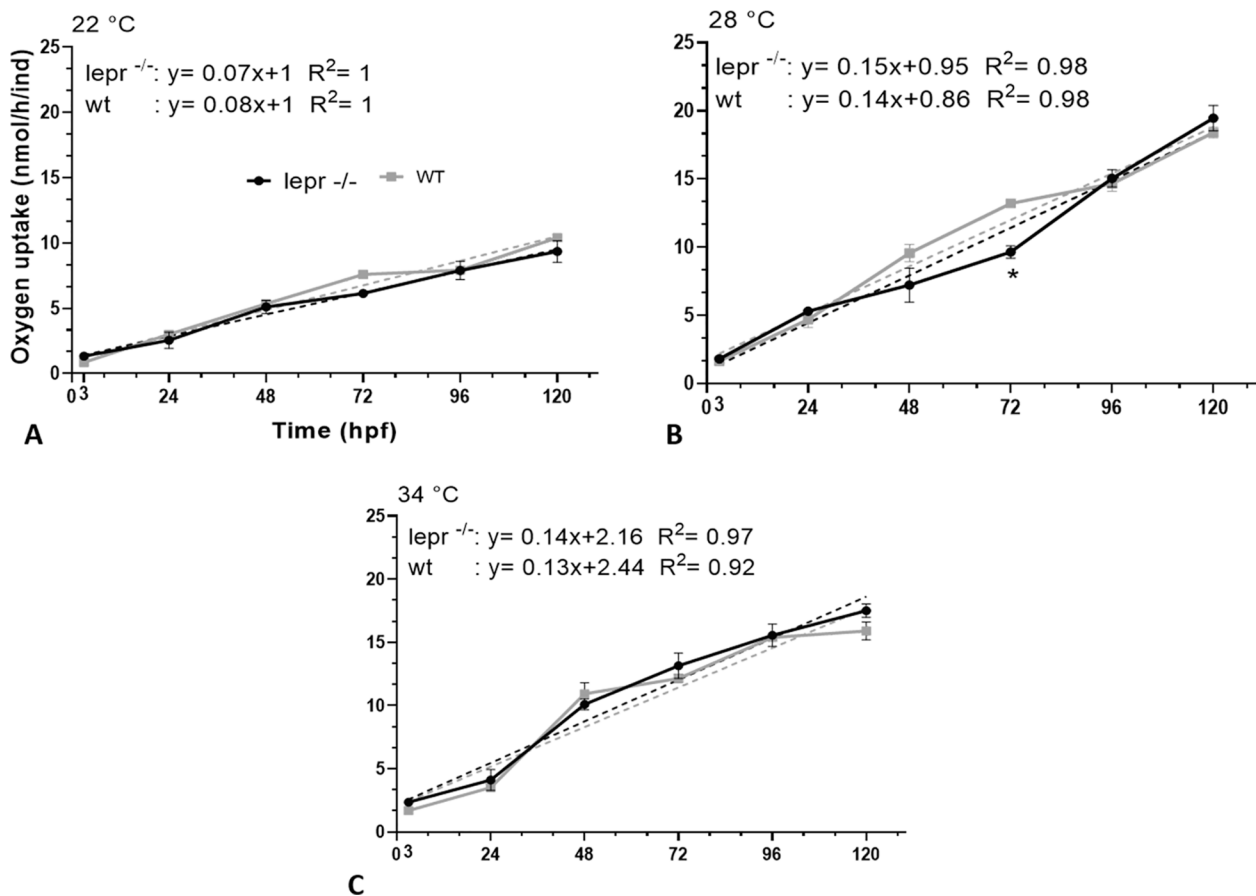
Fig. 2. Oxygen uptake in *lepr*$^{-/-}$ *vs. wt* embryos/early larvae at 22 (A), 28 (B) and 34 (C) °C from 3 to 120 hpf (endogenous feeding period). Each time-point is the mean of 6 vials, each containing 10 embryos (±SE). Two-way ANOVA shows significant effect of developmental age [F (5, 53) = 115.2; $p < 0.0001$] but not genotype [F (1, 53) = 3.342; $p > 0.05$] at 22 °C; significant effect of developmental age [F (5, 56) = 201.1; $p < 0.0001$] but not genotype [F (1, 56) = 2.779; $p > 0.05$] at 28 °C; significant effect of developmental age [F (5, 54) = 164.7; $p < 0.0001$] but not genotype [F (1, 54) = 2.102; $p > 0.05$] at 34 °C. A *post-hoc* Turkey's multiple comparison was used to assess specific pairwise differences (* = $p < 0.05$).

not show any differences in oxygen uptake in *lepr*$^{-/-}$ *vs. wt* fish (slopes equal to 0.07 and 0.08 at 22 °C; 0.15 and 0.14 at 28 °C; and 0.14 and 0.13 at 34 °C for *lepr*$^{-/-}$ and *wt*, respectively), with a single exception at 72 hpf. In fact, at this time-point, oxygen uptake at 28 °C was significantly lower in *lepr*$^{-/-}$ early larvae than that in *wt* (9.64 ± 0.45 nmol/h/individual and 13.2 ± 0.08 nmol/h/individual for *lepr*$^{-/-}$ and *wt*, respectively; $p < 0.05$).

Calculations of Q$_{10}$ (Table 1) and Ea (Table 2) values, as a response of oxygen rate consumption to two different and abrupt changes in water temperature (22–28 °C and 28–34 °C), showed some limited differences between the *lepr*$^{-/-}$ and *wt* lines. In particular, in the 22–28 °C temperature range, both *lepr*$^{-/-}$ and *wt* fish showed Q$_{10}$ > 2, with exceptions at two time-points for *lepr*$^{-/-}$ (Q$_{10}$ = 1.68 and Q$_{10}$ = 1.78 at 3 and 48 hpf, respectively). Conversely, in the 28–34 °C temperature range, both

fish lines showed Q$_{10}$ < 2; however, the Q$_{10}$ values were generally higher in *lepr*$^{-/-}$ than in *wt*. Notably, Q$_{10}$ < 1 values were also observed: Q$_{10}$ = 0.65 and 0.62 at 24 hpf for *lepr*$^{-/-}$ and *wt*, respectively; Q$_{10}$ = 0.87 at 72 hpf for *wt*; and Q$_{10}$ = 0.84 and 0.78 at 120 hpf for *lepr*$^{-/-}$ and *wt*, respectively. For E_a, in the 28–34 °C temperature range, negative values were generally calculated for both lines, with low incidence for the *lepr*$^{-/-}$ line (–32.857 and –13.611 KJ/mol at 24 and 120 hpf, respectively, for *lepr*$^{-/-}$; –4.639, –36.964, –19.669, and –18.816 KJ/mol at 3, 24, 72, and 120 hpf, respectively, for *wt*). In general, with respect to *wt*, the *lepr*$^{-/-}$ line exhibited comparable Q$_{10}$ and E_a values within the 22–28 °C temperature range and slightly higher values within the 28–34 °C temperature range.

Table 1
Comparison of Q$_{10}$ between *lepr*$^{-/-}$ and *wt* embryos at 3, 24, 48, 72, 96 and 120 hpf (endogenous feeding period). Q$_{10}$ was calculated at two temperature ranges (22–28 °C and 28–34 °C).

	3 hpf		24 hpf		48 hpf	
	22–28 °C	28–34 °C	22–28 °C	28–34 °C	22–28 °C	28–34 °C
lepr$^{-/-}$	1.68	1.54	3.41	0.65	1.78	1.75
wt	2.97	1.05	2.11	0.62	2.64	1.25
	72 hpf		96 hpf		120 hpf	
	22–28 °C	28–34 °C	22–28 °C	28–34 °C	22–28 °C	28–34 °C
lepr$^{-/-}$	2.13	1.68	2.93	1.06	3.39	0.84
wt	2.51	0.87	2.79	1.08	2.59	0.78

Table 2

Comparison of activation energy (E_a, KJ/mol) between $lepr^{-/-}$ and wt embryos at 3, 24, 48, 72, 96 and 120 hpf (endogenous feeding period). E_a was calculated at two temperature ranges (22–28 °C and 28–34 °C).

	3 hpf		24 hpf		48 hpf	
	22–28 °C	28–34 °C	22–28 °C	28–34 °C	22–28 °C	28–34 °C
$lepr^{-/-}$	38,458	33,313	90,563	−32,856	42,801	42,930
wt	80,370	−4,639	55,018	−36,964	71,718	17,127
	72 hpf		96 hpf		120 hpf	
	22–28 °C	28–34 °C	22–28 °C	28–34 °C	22–28 °C	28–34 °C
$lepr^{-/-}$	55,741	39,821	78,383	4,311	90,260	−13,611
wt	68,033	−10,669	75,791	6,158	70,338	−18,816

3.2.2. Evaluation of yolk-sac area in embryos/early larvae

The yolk-sac area served as an index for the utilization of endogenous resources. As shown in Fig. 3, the rate of yolk consumption during development was similar in $lepr^{-/-}$ and wt, with a single exception for 24 hpf, in which it was significantly lower in $lepr^{-/-}$ than in wt (0.210 ± 0.004 and 0.240 ± 0.010 mm² for $lepr^{-/-}$ and wt, respectively; $p < 0.05$).

3.2.3. Oxygen uptake in larvae/juveniles

Oxygen uptake analysis during the larval and juvenile stages (after the onset of exogenous feeding) was performed at the standard rearing temperature (28 °C). Oxygen consumption was analyzed every seven days, starting from 5 to 40 dpf. In both $lepr^{-/-}$ and wt lines, oxygen consumption increased during fish growth (Fig. 4), with significant differences observed for larvae (Fig. 4A) at 12 dpf (53.43 ± 2.07 and 27.12 ± 0.77 nmol/h/individual for $lepr^{-/-}$ and wt, respectively; $p < 0.0001$) and juveniles (Fig. 4B) at 40 dpf (35.86 ± 4.97 and 16.71 ± 3.02 nmol/h/mg for $lepr^{-/-}$ and wt, respectively; $p < 0.0001$). In these cases, the knockout line showed almost double oxygen consumption levels with respect to wt (see also Supplementary Table 2).

3.2.4. Monitoring of growth rate in larvae/juveniles

The fish were fed from 5 dpf, which marks the readiness and normal onset of exogenous feeding. At this time, the SL of $lepr^{-/-}$ and wt zebrafish were approximately similar (Fig. 5A); however, the knockout line appeared significantly longer than wt at 12 dpf (5.14 ± 0.02 and 3.60 ± 0.03 mm for $lepr^{-/-}$ and wt, respectively; $p < 0.01$). No differences were observed from 26 dpf and onwards, possibly indicating a slowdown in the knockout growth rate. For WW (Fig. 5B) and K (Table 3) analyses, data from fish at 26, 33, and 40 dpf were collected.
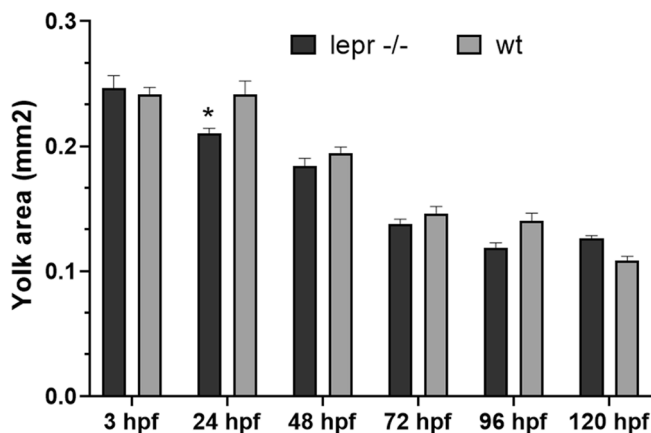

Fig. 3. Comparison of the yolk-sac area between $lepr^{-/-}$ and wt embryos/early larvae from 3 to 120 hpf (endogenous feeding period). Each time-point is the mean of 10–15 embryos (±SE). Two-way ANOVA shows significant effects of developmental age [F (5, 152) = 134.5; $p < 0.0001$] and genotype [F (1, 152) = 4.748; $p < 0.05$]. A post-hoc Turkey's multiple comparison was used to assess specific pairwise differences (* = $p < 0.05$).

Comparison between the two fish groups during the exogenous feeding period showed no significant differences in both analyses.

3.3. Effects of tube-fed administration of protein hydrolysate

3.3.1. Transcriptional expression analysis of appetite control-related genes in the larval head region

Analysis of 8 dpf larvae fasted for 18 h (unfed, untreated control), sampled at 0 h, administered a bolus containing lactalbumin hydrolysate (0%, 1%, 5%, and 15%, w/w), and sampled at 1 and 3 h post-administration showed differential gene expression responses in $lepr^{-/-}$ and wt lines (Fig. 6). In the larval head region, the mRNA expression levels of the fasted individuals (0 h) were significantly higher in $lepr^{-/-}$ than in wt larvae for npy (Fig. 6A), $cart$ (Fig. 4B), and $mc4r$ (Fig. 4D), but not for $agrp$ (Fig. 6C), for which comparable levels were recorded in the mutant and control fish.

After hydrolysate administration, npy mRNA (Fig. 6A) levels were downregulated in $lepr^{-/-}$ larvae at both 1 and 3 h post-administration, whereas mRNA levels were upregulated in wt at both time-points. However, a gradual concentration-dependent (from 0 to 15% protein hydrolysate) npy upregulation was present at both 1 and 3 h post-administration in $lepr^{-/-}$, while a substantial concentration-independent (from 0 to 15% protein hydrolysate) trend at 1 h and concentration-dependent (from 0% to 15% protein hydrolysate) down-regulation at 3 h post-administration was observed in wt. Further, $agrp$ mRNA (Fig. 6C) levels were downregulated in $lepr^{-/-}$ at both 1 and 3 h post-administration, whereas mRNA levels were upregulated in wt at both time-points. In $lepr^{-/-}$, significant concentration-dependent (from 0 to 15% protein hydrolysate) reductions in $agrp$ mRNA levels were observed at both 1 and 3 h post-administration, whereas an opposite trend of concentration-dependent (from 0 to 15% protein hydrolysate) upregulation was observed in wt at both time-points. After hydrolysate administration, $cart$ (Fig. 6B) mRNA levels exhibited concentration-dependent (from 0 to 15% protein hydrolysate) upregulation in both $lepr^{-/-}$ and wt larvae at 1 and 3 h post-administration. However, although an effect of protein hydrolysate administration could be seen in $lepr^{-/-}$ samples at high concentrations, with a more evident effect at 1 h, no evident protein hydrolysate concentration dependence on $cart$ was observed in wt. Finally, $mc4r$ (Fig. 6D) mRNA levels showed rather limited changes in $lepr^{-/-}$ and wt larvae at both 1 and 3 h. However, while $mc4r$ upregulation was observed in $lepr^{-/-}$ larvae at maximal (15%) protein hydrolysate levels at both 1 and 3 h, limited $mc4r$ upregulation was found in wt at low protein hydrolysate levels. For a time-dependent analysis of the above data, see Supplementary Fig. 2.

3.3.2. Transcriptional expression analysis of intestinal nutrient-sensing related genes in the larval trunk region

In the larval trunk section, $casr$ (Fig. 7A), $pept1b$ (Fig. 7C), $t1r1$ (Fig. 7D), $t1r2-1$ (Fig. 7E), $t1r2-2$ (Fig. 7F), and $t1r3$ (Fig. 7G) mRNA expression levels in the $lepr^{-/-}$ fasted larvae (0 h) were not significantly different from those in wt larvae. However, $pept1a$ (Fig. 7B) expression level appeared significantly higher in $lepr^{-/-}$ than in wt.
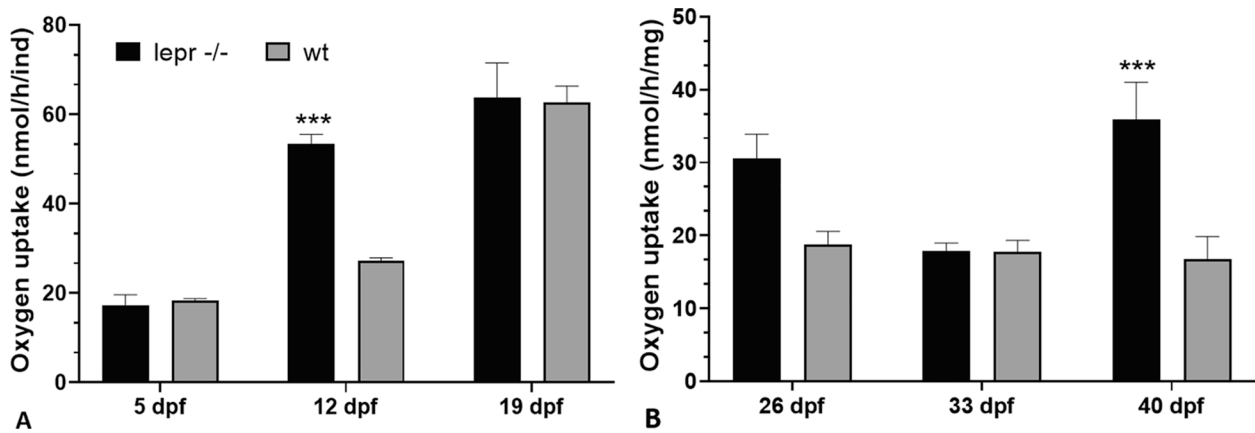
Fig. 4. (A) Comparison of oxygen uptake between $lepr^{-/-}$ and wt larvae at 28 °C from 5 to 19 dpf (exogenous feeding period). Each time-point is the mean of 6 vials, each containing 8–10 larvae (±SE). (B) Comparison of oxygen uptake/wet weight between $lepr^{-/-}$ and wt juveniles at 28 °C from 26 to 40 dpf (exogenous feeding period). Each time-point is the mean of 15 vials, each containing 1 juvenile (±SE). The number of fish per vial was chosen according to age and size. Two-way ANOVA shows significant effects of developmental age [F (2, 29) = 66.45; $p < 0.0001$] and genotype [F (1, 29) = 7.606; $p < 0.01$] for oxygen uptake in the 5–19 dpf range and significant effects of developmental age [F (2, 79) = 4.27; $p < 0.05$] and genotype [F (1, 79) = 16.29; $p < 0.0001$] for oxygen uptake/wet weight in the 26–40 dpf range. A *post-hoc* Turkey's multiple comparison was used to assess for specific pairwise differences (*** = $p < 0.001$). For detailed information see Supplementary Table 2.
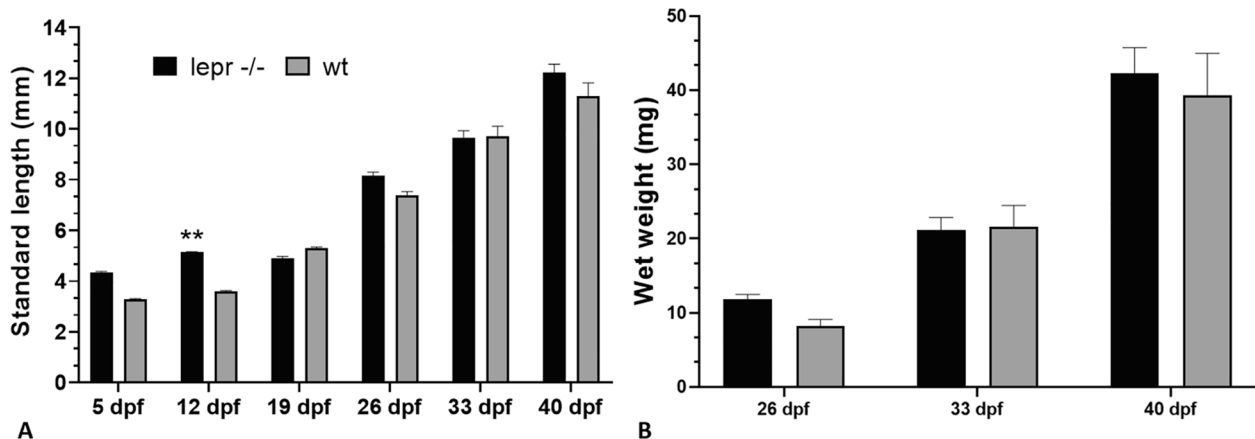

Fig. 5. (A) Comparison of the standard length between $lepr^{-/-}$ and wt larvae/juveniles from 5 to 40 dpf (exogenous feeding period). (B) Comparison of the wet weight between $lepr^{-/-}$ and wt juveniles from 26 to 40 dpf (exogenous feeding period). Each time-point is the mean of 10–15 fish (±SE). Two-way ANOVA shows significant effects of developmental age [F (5, 145) = 289.3; $p < 0.0001$] and genotype [F (1, 145) = 17.47: $p < 0.0001$] for standard length and a significant effect of developmental age [F (2, 84) = 50.45; $p < 0.0001$], but not genotype [F (1, 84) = 0.6449; $p > 0.05$] for wet weight. A *post-hoc* Turkey's multiple comparison was used to assess for specific pairwise differences (** = $p < 0.01$).

Table 3
Condition factor values for $lepr^{-/-}$ and wt juveniles from 26 to 40 dpf (exogenous feeding period). Each time-point is the mean of 15 fish (±SE). Two-way ANOVA shows a significant effect of developmental age [F (2, 81) = 32.37; $p < 0.0001$], but not genotype [F (1, 81) = 0.0003324; $p > 0.05$]. A *post-hoc* Turkey's multiple comparison was used to assess for specific pairwise differences.

	$lepr^{-/-}$		wt	
	Mean	SE	Mean	SE
26 dpf	2.09	0.05	1.96	0.04
33 dpf	2.22	0.03	2.26	0.04
40 dpf	2.34	0.04	2.42	0.07

In the case of *casr* (Fig. 7A), protein hydrolysate administration stimulated mRNA expression in both $lepr^{-/-}$ and wt larvae at both 1 and 3 h time-points; however, the stimulation did not appear to be concentration-dependent. As expected (Vacca et al., 2019), the mRNA expression levels of *pept1a* (Fig. 7B) paralleled those of *pept1b* (Fig. 7C) but with values approximately 25% lower under any experimental condition. In this case, the mRNA levels of both *pept1a* (Fig. 7B) and *pept1b* (Fig. 7C) were downregulated in $lepr^{-/-}$ and wt larvae at both 1 and 3 h, with $lepr^{-/-}$ mRNA levels invariably higher than those of wt at almost all time-points. In particular, in both $lepr^{-/-}$ and wt, decrease in mRNA expression levels was clearly concentration-dependent (from 0% to 15% protein hydrolysate) for both genes at 1 and 3 h. For the taste receptor genes, *t1r1* (Fig. 7D), *t1r2-1* (Fig. 7E), *t1r2-2* (Fig. 7F), and *t1r3* (Fig. 7G), different trends were observed. In particular, for *t1r1* (Fig. 7D), protein hydrolysate administration resulted in concentration-dependent (from 0% to 15% protein hydrolysate) upregulation and downregulation of $lepr^{-/-}$ and wt larvae, respectively, at 1 h, and similar trends were observed at 3 h. For *t1r2-1* (Fig. 7E), protein administration resulted in robust concentration-dependent (from 0% to 15%) down-regulations in both $lepr^{-/-}$ and wt larvae at 1 and 3 h, with a particularly evident effect in the knockout line at 3 h. Further, for *t1r2-2* (Fig. 7F), substantial concentration-independent increases were observed in $lepr^{-/-}$ larvae at both 1 and 3 h, whereas concentration-dependent decreases were observed in wt at both 1 and 3 h. Finally, for *t1r3* (Fig. 7G), limited concentration-dependent downregulation was observed in both $lepr^{-/-}$
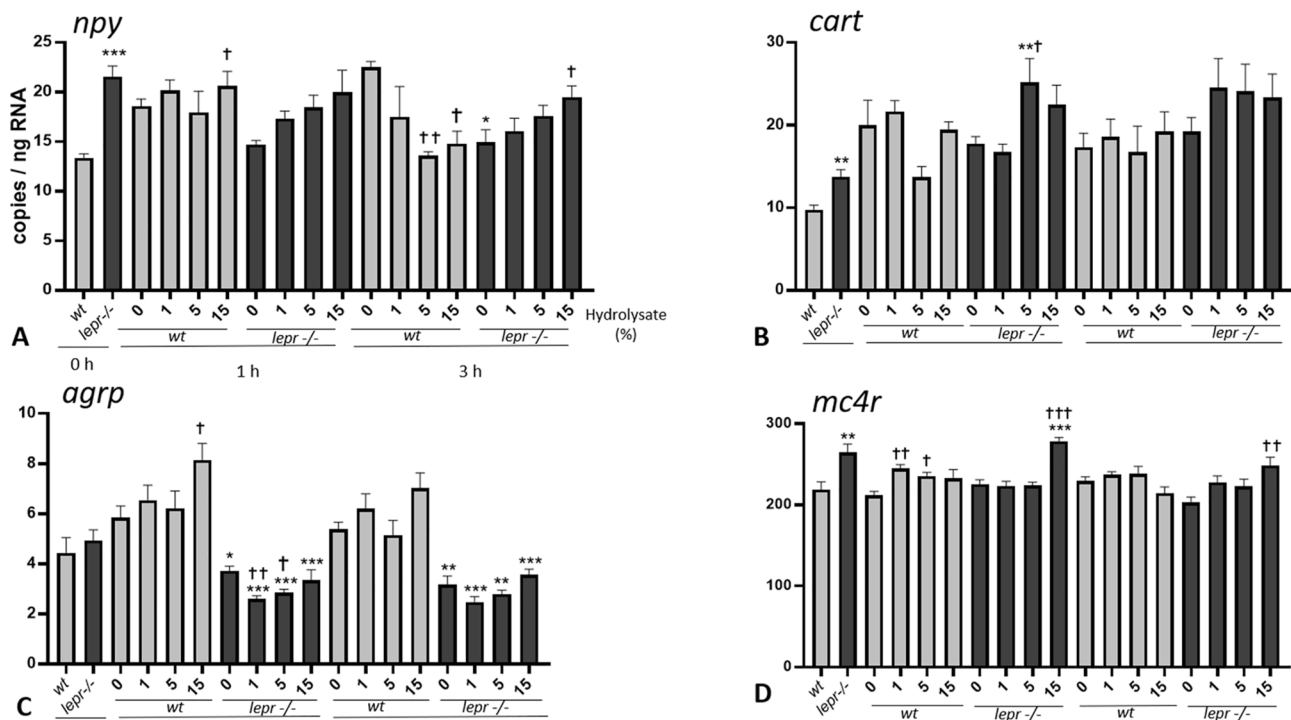
Fig. 6. (A-D). Effect of lactalbumin hydrolysate administration on appetite related genes in larval head (8 dpf). Values are mean ± SE ($n = 8$). Differences in tube-feeding test with respect to the values on the 0% hydrolysate group (indicated by †) within each zebrafish line ($lepr^{-/-}$ or wt) were assessed by one-way ANOVA. Differences between the lines at each sampling time (indicated by *) were assessed by two-way ANOVA. Two-way ANOVA shows no significant effects of concentration [$F (3, 55) = 2.311; p > 0.05$] and genotype [$F (1, 55) = 2.956; p > 0.05$] at 1 h and no significant effects of concentration [$F (3, 55) = 1.466; p > 0.05$] and genotype [$F (1, 55) = 0.004; p > 0.05$] at 3 h for *npy*; no significant effects of concentration [$F (3, 56) = 0.4654; p > 0.05$] and genotype [$F (1, 56) = 1.874; p > 0.05$] at 1 h and no significant effect of concentration [$F (3, 56) = 0.6222; p > 0.05$] but significant effect of genotype [$F (1, 56) = 6.588; p < 0.05$] at 3 h for *cart*; significant effects of concentration [$F (3, 56) = 3.010; p < 0.05$] and genotype [$F (1, 56) = 118.6; p < 0.0001$] at 1 h and significant effects of concentration [$F (3, 56) = 3.735; p < 0.05$] and genotype [$F (1, 56) = 100.4; p < 0.0001$] at 3 h for *agrp*; significant effect of concentration [$F (3, 56) = 14.43; p < 0.0001$] but no significant effect of genotype [$F (1, 56) = 2.571; p > 0.05$] at 1 h and no significant effects of concentration [$F (3, 56) = 1.912; p > 0.05$] and genotype [$F (1, 56) = 0.6626; p > 0.05$] at 3 h for *mc4r*. A Dunnett's multiple comparison test for one-way ANOVA and a *post-hoc* Turkey's multiple comparison were used to assess for specific pairwise differences (*, † = $p < 0.05$; **, †† = $p < 0.01$ and ***, ††† = $p < 0.001$).

and *wt* larvae at 1 and 3 h. For a time-dependent analysis of the above data, see Supplementary Fig. 3.

3.3.3. Transcriptional expression analysis of digestion- and absorption-related genes in the larval trunk region

In the larval trunk region, significantly higher mRNA expression levels of *ccka* (Fig. 8A), *cckb* (Fig. 8B), *pyyb* (Fig. 8D), *try* (Fig. 8E), *ct* (Fig. 8F), and *amy* (Fig. 8G) were recorded in $lepr^{-/-}$ fasted larvae compared with those in *wt*. Further, comparable levels were found in knockout and control lines for *pyya* (Fig. 8C).

In the case of *ccka* (Fig. 8A), protein hydrolysate administration induced limited changes in mRNA expression levels in $lepr^{-/-}$ larvae at both 1 and 3 h post-administration, while significant upregulation was observed at both time-points in *wt* larvae. In particular, no concentration-dependent effects were found at both 1 and 3 h in $lepr^{-/-}$, while evident concentration-dependent (from 0 to 15% protein hydrolysate) downregulation was observed at both 1 and 3 h in *wt*. For *cckb* (Fig. 8B), protein hydrolysate administration induced upregulation in $lepr^{-/-}$ and *wt* larvae at both 1 and 3 h. However, while concentration-dependent (from 0 to 15% protein hydrolysate) increases in the mRNA levels associated with $lepr^{-/-}$ (with a consistent effect observed at 15%) were observed at both 1 and 3 h, decreases associated with *wt* (with a consistent effect observed at 15%) were found at the same time-points. For *pyya* (Fig. 8C), protein hydrolysate induced upregulation in $lepr^{-/-}$ and *wt* larvae at both 1 and 3 h. In detail, the passage from 0 to 15% protein hydrolysate resulted in limited effect at 1 h and an evident increase in the mRNA levels in $lepr^{-/-}$ larvae, whereas similar administration resulted in consistent concentration-dependent reductions in the

mRNA levels in *wt* larvae, at both 1 and 3 h. For *pyyb* (Fig. 8D), the administration resulted in downregulation in $lepr^{-/-}$ at 1 and 3 h, while no clear effects were observed in *wt* at both time-points. In particular, the significant reductions in the mRNA levels in $lepr^{-/-}$ at both 1 and 3 h did not appear to be concentration-dependent, neither did the weak effect measured at both time-points. Further, for *try* (Fig. 8E), the administration of protein hydrolysate induced downregulation at both 1 and 3 h in $lepr^{-/-}$, while downregulation was evident at 3 h but not at 1 h in *wt*. Concentration-dependent increase in the mRNA levels was observed at high protein hydrolysate concentrations (15%) in $lepr^{-/-}$ at both 1 and 3 h, while a concentration-dependent decrease was observed in *wt* at 3 h, with no substantial changes at 1 h. For *ct* (Fig. 8F), a trend substantially similar to that of *try* was observed under the various experimental conditions. Analogously, *amy* mRNA expression levels (Fig. 8G) were substantially higher in $lepr^{-/-}$ than those in *wt*, substantially similar to those in the respective fasted controls. For a time-dependent analysis of the above data, see Supplementary Fig. 4.

4. Discussion

Leptin function in metabolism has been well described in mammals, and the concept that leptin plays a major role in the control of food intake and energy metabolism and that leptin receptor mediates these effects has been widely accepted. However, less is known about this function in fish and, in general, in non-mammalian species. Here, we aimed to explore the role of leptin receptor in energy allocation (metabolism) and nutrient acquisition (appetite, digestion, and absorption) using a recently generated zebrafish homozygous $lepr^{-/-}$
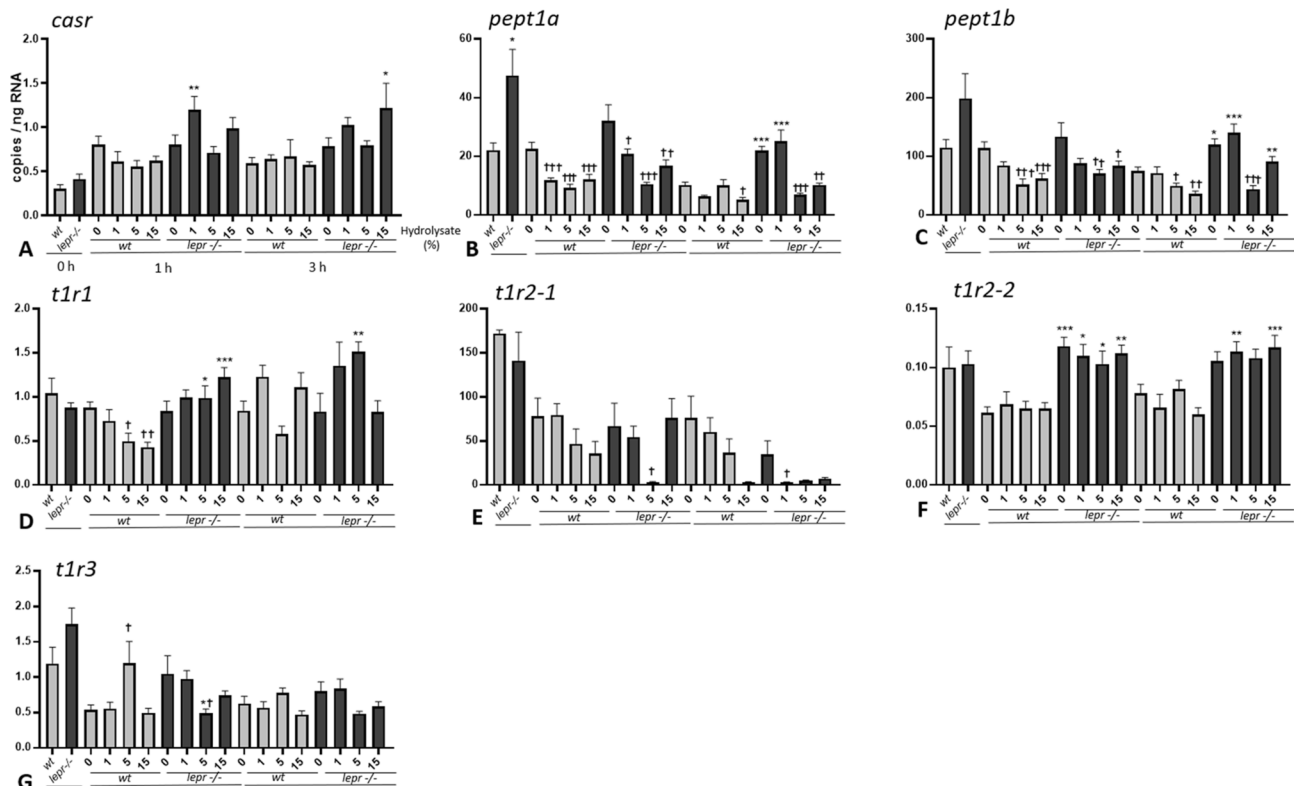
Fig. 7. (A-G). Effect of lactalbumin hydrolysate administration on nutrient-sensing related genes in larval trunk (8 dpf). Values are mean $\pm$ SE ($n = 8$). Differences in tube-feeding test with respect to the values on the 0% hydrolysate group (indicated by †) within each zebrafish line ($lepr^{-/-}$ or wt) were assessed by one-way ANOVA. Differences between the lines at each sampling time (indicated by *) were assessed by two-way ANOVA. Two-way ANOVA shows no significant effect of concentration [F (3, 53) = 2.292; $p > 0.05$] but significant effect of genotype [F (1, 53) = 14.30; $p < 0.0001$] at 1 h, and no significant effect of concentration [F (3, 54) = 0.9335; $p > 0.05$] but significant effect of genotype [F (1, 54) = 11.70; $p < 0.01$] at 3 h for $casr$; significant effects of concentration [F (3, 56) = 12. 14; $p < 0.0001$] and genotype [F (1, 56) = 7.005; $p < 0.05$] at 1 h and significant effects of concentration [F (3, 56) = 13.92; $p < 0.0001$] and genotype [F (1, 56) = 35.26; $p < 0.0001$] at 3 h for $pept1a$; significant effect of concentration [F (3, 56) = 10.91; $p < 0.0001$], but not genotype [F (1, 56) = 3.658; $p > 0.05$] at 1 h and significant effects of concentration [F (3, 56) = 20.15; $p < 0.0001$] and genotype [F (1, 56) = 42.18; $p < 0.0001$] at 3 h for $pept1b$; no significant effect of concentration [F (3, 56) = 0.5851; $p > 0.05$], but significant effect of genotype [F (1, 56) = 26.76; $p < 0.0001$] at 1 h and no significant effects of concentration [F (3, 55) = 2.728; $p > 0.05$] and genotype [F (1, 55) = 2.754; $p > 0.05$] at 3 h for $t1r1$; no significant effects of concentration [F (3, 52) = 2.435; $p > 0.05$] and genotype [F (1, 52) = 0.5828; $p > 0.05$] at 1 h and significant effects of concentration [F (3, 49) = 3.988; $p < 0.05$] and genotype [F (1, 49) = 8.861; $p < 0.01$] at 3 h for $t1r2$-1; no significant effect of concentration [F (3, 56) = 0.2170; $p > 0.05$] but significant effect of genotype [F (1, 56) = 64.26; $p < 0.0001$] at 1 h and no significant effect of concentration [F (3, 54) = 0.1986; $p > 0.05$] but significant effect of genotype [F (1, 54) = 43.93; $p < 0.0001$] at 3 h for $t1r2$-2; no significant effects of concentration [F (3, 53) = 0.7686; $p > 0.05$] and genotype [F (1, 53) = 1.129; $p > 0.05$] at 1 h and no significant effects of concentration [F (3, 55) = 1.748; $p > 0.05$] and genotype [F (1, 55) = 1.063; $p > 0.05$] at 3 h for $t1r3$. A Dunnett's multiple comparison test for one-way ANOVA and a *post-hoc* Turkey's multiple comparison were used to assess for specific pairwise differences (*, † = $p < 0.05$; **, †† = $p < 0.01$ and ***, ††† = $p < 0.001$).

mutant. The interpretation of the results needs to be done with some caution, since a single mutant line was expanded and used for all assays, and a backcross strategy was not employed. Therefore, it is unclear if a CRISPR off target may have influenced the results. Furthermore, although we confirmed that the *lepr* genomic mutation was actually transcribed, the impact of the protein has not been tested.

As we generated the new $lepr^{-/-}$ line, we first characterized it (embryonic, larval, and juvenile stages) based on oxygen uptake, as an index of energy use, and morphometry, as an index of energy allocation of endogenous and exogenous resources and growth during development. Oxygen uptake was comparable in developing $lepr^{-/-}$ and wt embryos and early larvae from 3 to 120 hpf (endogenous feeding period), although a significant decrease was observed at 72 hpf, that is, the endpoint of the embryonic and beginning of the early larval stage (Kimmel et al., 1995), at 28 °C, in $lepr^{-/-}$, indicating a possible stage of reduced metabolic activity. Interestingly, this was not associated with a depletion of the yolk resources in $lepr^{-/-}$ *vs wt* fish. Notably, the analysis of *lepr* gene expression in developing zebrafish carried out by Liu and colleagues. (2010) showed a significant increase at 72 hpf, and reduced *lepa* gene expression was detected at this time-point (Liu et al., 2012). Collectively, these data suggest that the roles of *lepr* and *lepa* in early

development involve a key functional point at 72 hpf, which is consistent with our evidence of reduced metabolic (oxygen uptake) activity. Such a question deserves specific analyses. The proposal that 72 hpf is a key point for *lepr* and *lepa* activities also agrees with results on reduced activity (Dalman et al., 2013) and transcriptional analyses of regulating genes (Tuttle et al., 2019) in a zebrafish *lepa* knockdown line compared to *wt* and rescued larvae at 72 hpf.

Q_{10}, which describes the zebrafish metabolic sensitivity to acute changes in water temperature, showed different responses when embryos and early larvae were transferred to lower (22 °C) or higher (34 °C) than the standard (28 °C) rearing temperature. Notably, in the 22–28 °C temperature range, both $lepr^{-/-}$ and wt had Q_{10} values > 2, which indicates comparable and positive dependence on temperature. In the 28–34 °C range, Q_{10} values were < 2 in both lines, indicating a slowdown of oxygen uptake rates. The same trend was observed in E_a, for which negative values were recorded in the 28–34 °C range. These findings suggest that 34 °C represents stressful conditions for embryos and early larvae, whereas no negative state occurs when they are reared at low temperatures (such as 22 °C). However, *lepr* does not seem to be involved in acute adjustments of metabolic rates when fish are exposed to different temperatures.
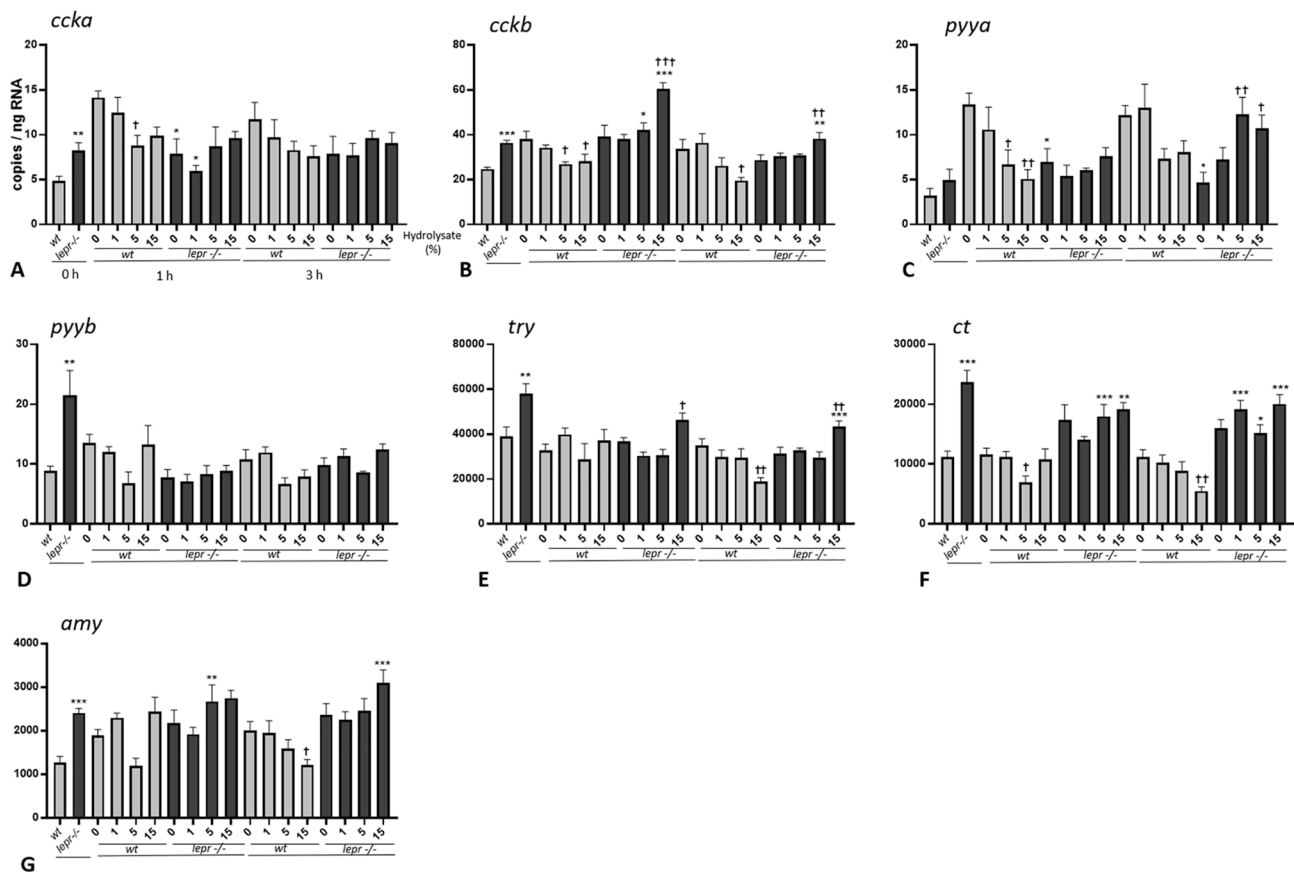
Fig. 8. (A-G). Effect of lactalbumin hydrolysate administration on digestion and absorption related genes in larval trunk (8 dpf). Values are mean ± SE ($n = 8$). Differences in tube-feeding test with respect to the values on the 0% hydrolysate group (indicated by †) within each zebrafish line ($lepr^{-/-}$ or wt) were assessed by one-way ANOVA. Differences between the lines at each sampling time (indicated by *) were assessed by two-way ANOVA. Two-way ANOVA shows no significant effect of concentration [$F_{(3, 48)} = 1.085; p > 0.05$] but significant effect of genotype [$F_{(1, 48)} = 12.07; p < 0.01$] at 1 h and no significant effects of concentration [$F_{(3, 48)} = 0.3605; p > 0.05$] and genotype [$F_{(1, 48)} = 0.5396; p > 0.05$] at 3 h for *ccka*; significant effects of concentration [$F_{(3, 53)} = 3.643; p < 0.05$] and genotype [$F_{(1, 53)} = 35.53; p < 0.0001$] at 1 h and no significant effects of concentration [$F_{(3, 54)} = 1.226; p > 0.05$] and genotype [$F_{(1, 54)} = 2.163; p > 0.05$] at 3 h for *cckb*; significant effects of concentration [$F_{(3, 55)} = 3.122; p < 0.05$] and genotype [$F_{(1, 55)} = 5.575; p < 0.05$] at 1 h and no significant effects of concentration [$F_{(3, 56)} = 0.4206; p > 0.05$] and genotype [$F_{(1, 56)} = 1.593; p > 0.05$] at 3 for *pyya*; no significant effect of concentration [$F_{(3, 56)} = 1.655; p > 0.05$] but a significant effect of genotype [$F_{(1, 56)} = 8.044; p < 0.01$] at 1 h and significant effect of concentration [$F_{(3, 54)} = 4.045; p < 0.05$] but not of genotype [$F_{(1, 54)} = 2.308; p > 0.05$] at 3 h for *pyyb*; significant effect of concentration [$F_{(3, 55)} = 3.464; p < 0.05$] but not of genotype [$F_{(1, 55)} = 0.2529; p > 0.05$] at 1 h and no significant effect of concentration [$F_{(3, 56)} = 0.6295; p > 0.05$] but significant effect of genotype [$F_{(1, 56)} = 9.654; p < 0.01$] at 3 h for *try*; no significant effect of concentration [$F_{(3, 55)} = 1.443; p > 0.05$] but significant effect of genotype [$F_{(1, 55)} = 43.10; p < 0.0001$] at 1 h and no significant effect of concentration [$F_{(3, 56)} = 1.362; p > 0.05$] but significant effect of genotype [$F_{(1, 56)} = 78.56; p < 0.0001$] at 3 h for *ct*; significant effects of concentration [$F_{(3, 55)} = 4.853; p < 0.05$] and genotype [$F_{(1, 55)} = 6.070; p < 0.05$] at 1 h and no significant effect of concentration [$F_{(3, 56)} = 0.1714; p > 0.05$], but significant effect of genotype [$F_{(1, 56)} = 23.34; p < 0.0001$] at 3 h for *amy*. A Dunnett's multiple comparison test for one-way ANOVA and a *post-hoc* Turkey's multiple comparison were used to assess for specific pairwise differences (*, † = $p < 0.05$; **, †† = $p < 0.01$ and ***, ††† = $p < 0.001$).

The reduction of the yolk sac area is an index of the rate of nutrient utilization in support of growth and metabolism during early development, and we analyzed it as a morphometric parameter related to the endogenous feeding period. The analysis showed a highly similar trend in the two genotypes, although the average yolk-sac area appears slightly smaller in the $lepr^{-/-}$ line from 24 to 96 hpf. An inversion was then found at 120 hpf, that is, the key time in organogenesis when the intestine is functionally complete and ready for the switch from endogenous to exogenous feeding (Wallace and Pack, 2003; Wallace et al., 2005). This increased use of yolk in the knockout fish might be indicative of a fast utilization of the endogenous nutrients; however, differences in the initial quantity of maternal nutritive material need to be further explored. Notably, our results are in line with those of Liu and Colleagues. (2012), who found no particular differences in yolk sac size between $lepa^{-/-}$ and wt zebrafish, except for one significant difference at 49 hpf.

Oxygen uptake analysis was also performed from the time of first feeding to juvenile stages (5–40 dpf), when exogenous food is the only

source of nutrients (Wallace and Pack, 2003; Wallace et al., 2005), and fish have an exponential growth phase (Gómez-Requeni et al., 2010). Our data indicated that at 12 and 40 dpf, $lepr^{-/-}$ zebrafish (maintained at the standard temperature) consume more oxygen than that consumed by wt. To our knowledge, this is the first report of oxygen uptake analysis performed after 5 dpf in a zebrafish $lepr^{-/-}$ line. However, for wt, similar analyses have already been performed by Rombough and Drader (2009). These authors presented oxygen uptake rates at 26, 33, and 40 dpf per individual; however, they did not include normalization by weight. Thus, the observed differences between studies might be due to size differences related to size variations between groups, strains, possible amplification by husbandry, etc. We therefore calculated the metabolic rate as oxygen uptake per time per weight unit to obtain a more reproducible analysis. Keeping zebrafish in stagnant water and in small chambers will result in the accumulation of metabolic waste products and induced stress in actively swimming juveniles, and this may represent a potential source of errors. In spite of such considerations, our data on oxygen uptake are of the same order of magnitude measured by

others for zebrafish individuals of comparable developmental stages.

The morphometric analysis included *SL* for larvae and juvenile phases, and *WW* and *K* for the juvenile phase only. All the morphometric analyses performed showed highly similar trends in zebrafish *lepr*$^{-/-}$ *vs wt* individuals, indicating no significant differences in growth during the larval and juvenile phases. However, the condition factor *K* (Froese, 2006) exhibited high values for both lines (*K* > 2), indicating an allocation of growth based on weight gain than on length (i.e., fat fish *vs.* lean fish). Notably, our data agreed well with those reported by Michel et al. (2016), where no significant differences were found in the comparison between *lepr*$^{-/-}$ and *wt* zebrafish. Nevertheless, it is worth noting in this context that the statistical morphometric differences between *wt* and *lepr*$^{-/-}$ (Fei et al., 2017¸Yang et al., 2019) or *lepa* knockout (Audira et al., 2018) or diet-induced obese lines (Mania et al., 2017) could be found from the adult, sexually mature stage onward (~3 months post-fertilization, mpf).

After metabolic characterization of the *lepr*$^{-/-}$ line, we focused on how the lack of leptin receptor-mediated signaling affects some key genes involved in appetite, sensing, and/or digestion in the gut after the administration of a specific dietary protein challenge. For this purpose, zebrafish larvae (8 dpf, 18 h fasting) were fed with different concentrations (0, 1, 5, and 15%) of lactalbumin hydrolysate directly into the digestive tract *via* tube feeding. The advantage of this method is the increased standardization of the experimental design because it is possible to deliver a known dosage of a solution directly into the gut at a known time (Rønnestad et al., 2001).

Initially, we examined the transcriptional expression of genes involved in appetite control, a complex mechanism mainly located in the hypothalamus with pathways coordinating a response that regulates food intake and energy homeostasis processes that seems to be conserved throughout vertebrates (Rønnestad et al., 2017; Volkoff et al., 2005; Volkoff, 2016). *npy* and *agrp*, produced by npy/agrp neurons, are both potent orexigenic players that act as antagonists of melanocortin receptors (mc3r and mc4r) (Beck, 2006; Clark et al., 1984; Stanley and Leibowitz, 1985; Shutter et al., 1997), and their orexigenic effects have already been assessed in zebrafish (Song et al., 2003; Yokobori et al., 2012). Leptin interacts with their release inhibiting orexigenic systems in cypriniforms (Volkoff et al., 2003; Yan et al., 2016). This is supported by our data, in which the orexigenic *npy* mRNA level in the zebrafish mutant is significantly higher than that in *wt*, probably as a result of fasting and lack of inhibition by leptin. This finding has also been reported by other studies (see e.g., Ahi et al., 2019; Opazo et al., 2019) in parallel to the upregulation of the orexigenic *agrp*, which, on the contrary, did not show any significant differences in our study. However, in spite of their basal expression in the fasted state, both *npy* and *agrp* responded to the downregulation in *lepr*$^{-/-}$ and upregulation in *wt* upon oral administration of protein hydrolysate, suggesting the deregulation of the leptin receptor-mediated pathway in the mutant fish.

For *cart*, an anorexigenic factor produced by pomc/cart neurons that acts as an agonist of melanocortin receptors (Bagnol et al., 1999; Cowley et al., 1999) an increased mRNA levels in *lepr*$^{-/-}$ *vs. wt* fish in the fasted state was observed. In addition, post-feeding increases in *cart* expression in the brain have been reported in several fish species, such as catfish (*Ictalurus punctatus*) (Peterson et al., 2012), Atlantic salmon (Valen et al., 2011), and goldfish (Volkoff and Peter, 2001), suggesting that Cart acts as a short-term satiety factor in fish. In our system, both *lepr*$^{-/-}$ and *wt* larvae robustly responded to protein hydrolysate administration and such response became even stronger at high levels of protein hydrolysate administered in the *lepr*$^{-/-}$ mutant, suggesting a direct role of gut luminal proteins in the central control of the nutritional state. This is in contrast to the findings of another study (Ahi et al., 2019) in which both zebrafish *lepr* mutant and *wt* did not show any substantial variation of *cart* 2 and 6 h post-feeding, although in this study, fish were regularly fed with dry and live food. In addition, the expression of all four *cart* paralog genes, namely, *cart1*, *cart2*, *cart3*, and *cart4* (Akash et al., 2014), were studied in the paper by Ahi and colleagues. (2019), while our study

focused on *cart3* (NM_001327818).

Interestingly, *mc4r* mRNA levels of both fasted and protein hydrolysate administered *lepr*$^{-/-}$ and *wt* larvae had the same profile as that of *cart*, including the specific boost associated with the high levels of protein hydrolysate, which shows the importance of other appetite signaling pathways than leptin in the acquisition of proteins and amino acids in zebrafish larvae.

Next, we investigated the transcriptional expression of a set of genes involved in nutrient sensing in the digestive tract, a complex mechanism involving both local and remote signaling pathways involving the CNS (Rønnestad et al., 2014), including CASR, a C GPCR receptor involved in the control of food intake (Ojha, 2018) and the luminal sensing of aromatic amino acids and peptides (Broadhead et al., 2011; Conigrave et al., 2000; Conigrave and Brown, 2006; Mun et al., 2004; Quinn et al., 1997; Tang et al., 2016; Wang et al., 2006), the T1R family members, involved in mammalian nutrient luminal sensing of aliphatic non-essential L-amino acids and glutamate in the monosodium form (Morais, 2017; Rønnestad et al., 2014), and the H$^+$-coupled oligopeptide transporter PEPT1, a transporter of dietary di- and tripeptides in all vertebrates and a peptide chemosensor in mammals (Diakogiannaki et al., 2013; Daniel and Zietek, 2015; Liou et al., 2011; Matsumura et al., 2005; Rønnestad et al., 2014).

Analysis of *casr* mRNA levels indicated no difference in fasted *lepr*$^{-/-}$ and *wt* larvae. However, differences in the administered protein hydrolysate resulted in higher mRNA levels in mutants than in *wt*. Analogously, none of the *t1r* genes expressed differently in fasted *lepr*$^{-/-}$ or *wt* larvae; however, while *t1r1* and *t1r2-2* expressions showed some upregulation in the presence of protein hydrolysate, *t1r3* did not. Notably, in our experiments, the expression of *t1r2-1*, which is present in tandem in the zebrafish and grass carp genome (*Ctenopharyngodon idella*) (Yuan et al., 2020), was 2–3 orders of magnitude higher than those of other receptors and comparable to those of *pept1a* and *pept1b*, suggesting a large representation of *t1r2-1* mRNAs in the trunk section. Its specific localization is lacking in this study, and the involvement of structures other than the gut cannot be excluded, although it may suggest that this is a key nutrient sensor in the gut. *pept1a* and *pept1b* are paralog genes resulting from whole-genome duplication events in teleost fish (Con et al., 2017; Gonçalves et al., 2007). *pept1b* is regarded as a physiological marker of intestinal maturation, differentiation, and function in all vertebrates (Verri et al., 2003), while *pept1a* is less characterized, although it shows a functional expression comparable to *pept1b* (Gomes et al., 2020; Vacca et al., 2019). The transcriptional analysis of both peptide transporters showed an evident upregulation in fasted *lepr*$^{-/-}$ larvae (although not significant for *pept1b*) with respect to *wt*. In addition, a parallel trend in expression was observed for both genes after protein hydrolysate administration, with an evident time- and concentration-dependent downregulation in both lines, although *lepr*$^{-/-}$ showed significantly higher mRNA levels at 3 h than those in *wt* at almost all time-points. This finding adds to a previous suggestion in *wt* of an enhancement of peptide absorption by leptin through post-translation regulation (Buyse et al., 2001), thus facilitating the endocrine and/or paracrine actions of leptin system (Garcia-Suarez et al., 2018).

Lastly, we investigated the mRNA expression profile of genes mainly related to the digestive processes, which includes *cck*, a hormone stimulating the release of digestive enzymes such as *try*, *ct*, and *amy* (all investigated in this work) from the pancreas and bile from the gallbladder (Boguszewski et al., 2010; Dockray, 2012). In addition, we studied *pyy*, a hormone secreted by enteroendocrine L cells of the lower gastrointestinal tract that, in mammals, plays a key role in regulating parameters of energy and glucose metabolism (Zhang et al., 2012). Overall, both gut hormones are related to signaling satiety and inhibition of food intake in mammals (Abbott et al., 2005a, 2005b; Dockray, 2006), and leptin enhances the sensitivity to short-term satiety signals of both (Guilmeau et al., 2003; Raybould, 2007; Uniappan and Kieffer, 2008). In fish, this anorexigenic effect seems to be confirmed for *cck*,

whereas, for *pyy*, the function is not consistently observed across species (Volkoff, 2016).

In our experiments, *ccka*, *cckb*, *pyyb*, *try*, *ct*, and *amy*, but not *pyya*, mRNA levels were significantly higher in fasted *lepr*$^{-/-}$ than in fasted *wt* larvae. After protein hydrolysate administration, *ccka* and *cckb* mRNA levels decreased in a concentration- and time-dependent manner in *wt* larvae, while *cckb* mRNA levels significantly increased at high protein hydrolysate concentrations in *lepr*$^{-/-}$ larvae, suggesting a differential response to luminal protein. Analogously, while *pyya* and *pyyb* mRNA levels exhibited a tendency to decrease in *wt* larvae, *pyya* increased at high protein hydrolysate levels in *lepr*$^{-/-}$ larvae. These trends of *cckb* and *pyya* paralleled those of *try*, *ct*, and *amy*, in terms of concentration- and time-dependent decreases in *wt* and concentration- and time-dependent increases in *lepr*$^{-/-}$ larvae.

Moreover, only *pyyb* (in *lepr*$^{-/-}$), *try,* and *ct*, showed the expected reduced expression after protein hydrolysate administration, although higher levels than those in *wt* were found in response to fasting, whereas *cck*a, *cckb*, *pyyb*, and *amy* did not show reduced expression following administration. However, with high hydrolysate doses administered, while a hint of downregulation was observed in *wt*, an opposite regulation was shown in *lepr*$^{-/-}$, suggesting a possible leptin involvement with high protein concentration.

4.1. Conclusion

In summary, our analysis provides a characterization of the *lepr*$^{-/-}$ zebrafish mutant with respect to some key elements in energy allocation, metabolism, and nutrient acquisition. Comparison between *lepr*$^{-/-}$ and *wt* fish up to 40 dpf showed very minor differences in oxygen consumption and general morphometric parameters. Conversely, consistent differences emerged from the transcriptional analysis of a set of genes involved in the control of appetite, sensing, and digestion, both in the fasted state and, notably, after protein hydrolysate administration, which suggests that *lepr* may play a role in the regulation of dietary protein acquisition in zebrafish larvae. Focusing on the mechanisms that control appetite and food intake from first feeding larvae to juveniles requires special care in data analysis, due the fact that the physiological networks that support such regulatory functions may be immature in the early phases of development and differ from those in the post-metamorphic and adult stages. In addition, in the early developmental stages, orexigenic stimuli may largely prevail since fish larvae can be regarded as "feeding machines" as they can even sometimes continue to ingest food despite a full and distended gut, suggesting lack of satiation signals (Harboe et al., 2009). Zebrafish is an agastric species, with adaptations in its digestive physiology as well as a feeding biology that differs from that of gastric species, including mammals. This may explain some differential responses in terms of gene expression in the analyzed stages of zebrafish. However, our zebrafish *lepr*$^{-/-}$ mutant is a suitable model to learn more about the key signaling pathways involved in nutritional physiology, control of food intake and energy homeostasis, and allocation of growth in vertebrates.

Author contributions

The study was conceived by IR, KM, GdV. KM produced the *lepr*$^{-/-}$ zebrafish line. The experiment and lab analysis were executed by GdV and KM. Statistical analysis and related graphs done by KM, ASG, GdV, TV. GdV and TV prepared the first draft of the paper. All authors contributed to the interpretation of the data, writing of the manuscript, read and approved the submitted version.

Declaration of Competing Interest

The authors declare that they have no known competing financial interests or personal relationships that could have appeared to influence the work reported in this paper.

Author contributions

Appendix A. Supplementary data

Supplementary data to this article can be found online at https://doi.org/10.1016/j.ygcen.2021.113832.

References

Abbott, C.R., Monteiro, M., Small, C.J., Sajedi, A., Smith, K.L., Parkinson, J.R.C., Ghatei, M.A., Bloom, S.R., 2005a. The inhibitory effects of peripheral administration of peptide YY(3–36) and glucagon-like peptide-1 on food intake are attenuated by ablation of the vagal-brainstem-hypothalamic pathway. Brain. Res. 1044 (1), 127–131. https://doi.org/10.1016/j.brainres.2005.03.011.

Abbott, C.R., Small, C.J., Kennedy, A.R., Neary, N.M., Sajedi, A., Ghatei, M.A., Bloom, S.R., 2005b. Blockade of the neuropeptide Y Y2 receptor with the specific antagonist BIIE0246 attenuates the effect of endogenous and exogenous peptide YY(3–36) on food intake. Brain Res. 1043 (1-2), 139–144. https://doi.org/10.1016/j.brainres.2005.02.065.

Ahi, E.P., Brunel, M., Tsakoumis, E., Schimtz, M., 2019. Transcriptional study of appetite regulating genes in the brain of zebrafish (*Danio rerio*) with impaired leptin signaling. Sci. Rep. 9, 20166. https://doi.org/10.1038/s41598-019-56779-z.

Akash, G., Kaniganti, T., Tiwari, N.K., Subhedar, N.K., Ghose, A., 2014. Differential distribution and energy status-dependent regulation of the four CART neuropeptide genes in the zebrafish brain. J. Comp. Neurol. 522 (10), 2266–2285. https://doi.org/10.1002/cne.23532.

Angotzi, A.R., Stefansson, S.O., Nilsen, T.O., Rathore, R.M., Rønnestad, I., 2013. Molecular cloning and genomic characterization of novel leptin-like genes in salmonids provide new insight into the evolution of the leptin gene family. Gen. Comp. Endocrinol. 187, 48–59. https://doi.org/10.1016/j.ygcen.2013.03.022.

Ansai, S., Kinoshita, M., 2014. Targeted mutagenesis using CRISPR/Cas system in medaka. Biol. Open 3, 362–371. https://doi.org/10.1242/bio.20148177.

Audira, G., Sarasamma, S., Chen, J.R., Juniardi, S., Sampurna, B.P., Liang, S.T., Lai, Y.H., Lin, G.M., Hsieh, M.C., Hsiao, C.D., 2018. Zebrafish mutants carrying leptin a (lepa) gene deficiency display obesity, anxiety, less aggression and fear, and circadian rhythm and color preference dysregulation. Int. J. Mol. Sci. 19, 4038. https://doi.org/10.3390/ijms19124038.

Bagnol, D., Lu, X.Y., Kaelin, C.B., Day, H.E., Ollmann, M., Gantz, I., Akil, H., Barsh, G.S., Watson, S.J., 1999. Anatomy of an endogenous antagonist: relationship between Agouti-related protein and proopiomelanocortin in brain. J. Neurosci. 19, RC26. https://doi.org/10.1523/JNEUROSCI.19-18-j0004.

Banks, W.A., Coon, A.B., Robinson, S.M., Moinuddin, A., Shultz, J.M., Nakaoke, R., Morley, J.E., 2004. Triglycerides induce leptin resistance at the blood–brain barrier. Diabetes 53 (5), 1253–1260. https://doi.org/10.2337/diabetes.53.5.1253.

Beck, B., 2006. Neuropeptide Y in normal eating and in genetic and dietary-induced obesity. Philos. Trans. R. Soc. Lond. B. Biol. Sci. 361 (1471), 1159–1185. https://doi.org/10.1098/rstb.2006.1855.

Boguszewski, C.L., Paz-Filho, G., Velloso, L.A., 2010. Neuroendocrine body weight regulation: integration between fat tissue, gastrointestinal tract, and the brain. Endokrynol. Polska 61, 194–206.

Boston, B.A., Blaydon, K.M., Varnerin, J., Cone, R.D., 1997. Independent and additive effects of central POMC and leptin pathways on murine obesity. Science 278, 1641-1644. https://doi.org/10.1126/science.278.5343.1641.

Broadhead, G.K., Mun, H.C., Avlani, V.A., Jourdon, O., Church, W.B., Christopoulos, A., Delbridge, L., Conigrave, A.D., 2011. Allosteric modulation of the calcium-sensing receptor by gamma-glutamyl peptides: inhibition of PTH secretion, suppression of intracellular cAMP levels, and a common mechanism of action with L-amino acids. J. Biol. Chem. 286, 8786–8797. https://doi.org/10.1074/jbc.M110.149724.

Buyse, M., Berlioz, F., Guilmeau, S., Tsocas, A., Voisin, T., Péranzi, G., Merlin, D., Laburthe, M., Lewin, M.J.M., Rozé, C., Bado, A., 2001. PepT1-mediated epithelial transport of dipeptides and cephalexin is enhanced by luminal leptin in the small intestine. J. Clin. Invest. 108 (10), 1483–1494. https://doi.org/10.1172/JCI13219.

Chen, H., Charlat, O., Tartaglia, L.A., Woolf, E.A., Weng, X., Ellis, S.J., Lakey, N.D., Culpepper, J., More, K.J., Breitbart, R.E., Duyk, G.M., Tepper, R.I., Morgenstern, J. P., 1996. Evidence that the diabetes gene encodes the leptin receptor: identification of a mutation in the leptin receptor gene in db/db mice. Cell 84 (3), 491–495. https://doi.org/10.1016/S0092-8674(00)81294-5.

Chisada, S.-I., Kurokawa, T., Murashita, K., Rønnestad, I., Taniguchi, Y., Toyoda, A., Sakaki, Y., Takeda, S., Yoshiura, Y., 2014. Leptin receptor-deficient (knockout) medaka, Oryzias latipes, show chronical up-regulated levels of orexigenic neuropeptides, elevated food intake and stage specific effects on growth and fat allocation. Gen. Comp. Endocrinol. 195, 9–20.

Clark, J.T., Kalra, P.S., Crowley, W.R., Kalra, S.P., 1984. Neuropeptide Y and human pancreatic polypeptide stimulate feeding behavior in rats. Endocrinology 115 (1), 427–429. https://doi.org/10.1210/endo-115-1-427.

Con, P., Nitzan, T., Cnaani, A., 2017. Salinity dependent shift in the localization of three peptide transporters along the intestine of the Mozambique tilapia (*Oreochromis mossambicus*). Front. Physiol. 8 https://doi.org/10.3389/fphys.2017.00008.

Conigrave, A.D., Brown, E.M., 2006. Taste receptors in the gastrointestinal tract. II. L-amino acid sensing by calcium-sensing receptors: implications for GI physiology. Am. J. Physiol. Gastrointest. Liver. Physiol. 291, G753–G761. https://doi.org/10.1152/ajpgi.00189.2006.

Conigrave, A.D., Quinn, S.J., Brown, E.M., 2000. L-amino acid sensing by the extracellular Ca2+-sensing receptor. Proc. Natl. Acad. Sci. USA 97 (9), 4814–4819. https://doi.org/10.1073/pnas.97.9.4814.

Cowley, M.A., Pronchuk, N., Fan, W., Dinulescu, D.M., Colmers, W.F., Cone, R.D., 1999. Integration of NPY, AGRP, and melanocortin signals in the hypothalamic paraventricular nucleus: evidence of a cellular basis for the adipostat. Neuron. 24 (1), 155–163. https://doi.org/10.1016/S0896-6273(00)80829-6.

Dalman, M.R., Liu, Q., King, M.D., Bagatto, B., Londraville, R.L., 2013. Leptin expression affects metabolic rate in zebrafish embryos (D. rerio). Front. Physiol. 4, 160, 2013. https://doi.org/10.3389/fphys.2013.00160.

Daniel, H., Zietek, T., 2015. Taste and move: glucose and peptide transporters in the gastrointestinal tract. Exp. Physiol. 100 (12), 1441–1450. https://doi.org/10.1113/EP085029.

Diakogiannaki, E., Pais, R., Tolhurst, G., Parker, H.E., Horscroft, J., Rauscher, B., Zietek, T., Daniel, H., Gribble, F.M., Reimann, F., 2013. Oligopeptides stimulate glucagon-like peptide-1 secretion in mice through proton-coupled uptake and the calcium-sensing receptor. Diabetologia. 56 (12), 2688–2696. https://doi.org/10.1007/s00125-013-3037-3.

Dockray, G.J., 2006. Gastrointestinal hormones: cholecystokinin, somatostatin and ghrelin. In. Johnson, LR., editor Physiology of the Gastrointestinal Tract Vol. 1 Elsevier Academic Press: 91-120.

Dockray, G.J., 2012. Cholecystokinin. Curr. Opin. Endocrinol. Diabetes Obes. 19, 8-12. https://doi.org/10.1097/MED.0b013e32834eb77d.

Elias, C.F., Lee, C., Kelly, J., Aschkenasi, C., Ahima, R.S., Couceyro, P.R., Kuhar, M.J., Saper, C.B., Elmquist, J.K., 1998. Leptin activates hypothalamic CART neurons projecting to the spinal cord. Neuron 21 (6), 1375–1385. https://doi.org/10.1016/S0896-6273(00)80656-X.

Elias, C.F., Purohit, D., 2013. Leptin signaling and circuits in puberty and fertility. Cell. Mol. Life Sci. 70 (5), 841–862. https://doi.org/10.1007/s00018-012-1095-1.

Erickson, J.C., Clegg, K.E., Palmiter, R.D., 1996. Sensitivity to leptin and susceptibility to seizures of mice lacking neuropeptide Y. Nature. 381 (6581), 415–418. https://doi.org/10.1038/381415a0.

Fei, F., Sun, S.Y., Yao, Y.X., Wang, X., 2017. Generation and phenotype analysis of zebrafish mutations of obesity-related genes lepr and mc4r. Sheng Li Xue Bao: [Acta physiologica Sinica] 69, 61–69.

Froese, R., 2006. Cube law, condition factor and weight-length relationships: history, meta-analysis and recommendations. J. Appl. Ichthyol. 22 (4), 241–253. https://doi.org/10.1111/jai.2006.22.issue-410.1111/j.1439-0426.2006.00805.x.

Fruhbeck, G., 2006. Intracellular signalling pathways activated by leptin. Biochem. J. 393, 7–20. https://doi.org/10.1042/BJ20051578.

Garcia-Suarez, O., Cabo, R., Abbate, F., Randazzo, B., Laurà, R., Piccione, G., Germanà, A., Levanti, B., 2018. Presence and distribution of leptin and its receptor in the gut of adult zebrafish in response to feeding and fasting. Anat. Histol. Embryol. 47 (5), 456–465. https://doi.org/10.1111/ahe.2018.47.issue-510.1111/ahe.12384.

Gomes, A.S., Vacca, F., Cinquetti, R., Murashita, K., Barca, A., Bossi, E., Rønnestad, I., Verri, T., 2020. Identification and characterization of the Atlantic salmon peptide transporter 1a. Am. J. Physiol. Cell. Physiol. 318 (1), C191–C204. https://doi.org/10.1152/ajpcell.00360.2019.

Gómez-Requeni, P., Conceição, L.E.C., Olderbakk Jordal, A.-E., Rønnestad, I., 2010. A reference growth curve for nutritional experiments in zebrafish (Danio rerio) and

changes in whole body proteome during development. Fish. Physiol. Biochem. 36 (4), 1199–1215. https://doi.org/10.1007/s10695-010-9400-0.

Gonçalves, A.F., Castro, L.F.C., Pereira-Wilson, C., Coimbra, J., Wilson, J.M., 2007. Is there a compromise between nutrient uptake and gas exchange in the gut of Misgurnus anguillicaudatus, an intestinal air-breathing fish? Comp. Biochem. Physiol. Part D Genomics Proteomics 2 (4), 345–355. https://doi.org/10.1016/j.cbd.2007.08.002.

Gorissen, M., Bernier, N.J., Nabuurs, S.B., Flik, G., Huising, M.O., 2009. Two divergent leptin paralogues in zebrafish (Danio rerio) that originate early in teleostean evolution. J. Endocrinol. 201, 329–339. https://doi.org/10.1677/JOE-09-0034.

Gorissen, M., Flik, G., 2014. Leptin in teleostean fish, towards the origins of leptin physiology. J. Chem. Neuroanat. 61–62, 200–206. https://doi.org/10.1016/j.jchemneu.2014.06.005.

Guilmeau, S., Buyse, M., Tsocas, A., Laigneau, J.P., Bado, A., 2003. Duodenal leptin stimulates cholecystokinin secretion: evidence of a positive leptin-cholecystokinin feedback loop. Diabetes 52 (7), 1664–1672. https://doi.org/10.2337/diabetes.52.7.1664.

Harboe, T., Mangor-Jensen, A., Moren, M., Hamre, K., Rønnestad, I., 2009. Control of light condition affects the feeding regime and enables successful eye migration in Atlantic halibut juveniles. Aquaculture 290 (3-4), 250–255. https://doi.org/10.1016/j.aquaculture.2009.02.032.

Havel, P.J., 2004. Update on adipocyte hormones: regulation of energy balance and carbohydrate/lipid metabolism. Diabetes 53 (Supplement 1), S143–S151. https://doi.org/10.2337/diabetes.53.2007.S143.

Huising, M.O., Geven, E.J.W., Kruiswijk, C.P., Nabuurs, S.B., Stolte, E.H., Spanings, F.A. T., Verburg-van Kemenade, B.M.L., Flik, G., 2006. Increased leptin expression in common carp (*Cyprinus carpio*) after food intake but not after fasting or feeding to satiation. Endocrinology 147 (12), 5786–5797. https://doi.org/10.1210/en.2006-0824.

Hummel, K.P., Dickie, M.M., Coleman, D.L., 1966. Diabetes, a new mutation in the mouse. Science 153, 1127–1128. https://doi.org/10.1126/science.153.3740.1127.

Kimmel, C.B., Ballard, W.W., Kimmel, S.R., Ullmann, B., Schilling, T.F., 1995. Stages of embryonic development of the zebrafish. Dev. Dyn. 203 (3), 253–310. https://doi.org/10.1002/aja.1002030302.

Kristensen, P., Judge, M.E., Thim, L., Ribel, U., Christjansen, K.N., Wulff, B.S., Clausen, J. T., Jensen, P.B., Madsen, O.D., Vrang, N., Larsen, P.J., Hastrup, S., 1998. Hypothalamic CART is a new anorectic peptide regulated by leptin. Nature 393 (6680), 72–76. https://doi.org/10.1038/29993.

Kurokawa, T., Uji, S., Suzuki, T., 2005. Identification of cDNA coding for a homologue to mammalian leptin from pufferfish, Takifugu rubripes. Peptides 26 (5), 745–750. https://doi.org/10.1016/j.peptides.2004.12.017.

Kurokawa, T., Murashita, K., 2009. Genomic characterization of multiple leptin genes and a leptin receptor gene in the Japanese medaka, Oryzias latipes. Gen. Comp. Endocrinol. 161 (2), 229–237. https://doi.org/10.1016/j.ygcen.2009.01.008.

Kuroyanagi, M., Katayama, T., Imai, T., Yamamoto, Y., Chisada, S.-I., Yoshiura, Y., Ushijima, T., Matsushita, T., Fujita, M., Nozawa, A., Suzuki, Y., Kikuchi, K., Okamoto, H., 2013. New approach for fish breeding by chemical mutagenesis: establishment of TILLING method in fugu (Takifugu rubripes) with ENU mutagenesis. BMC Genomics 14 (1), 786. https://doi.org/10.1186/1471-2164-14-786.

Liou, A.P., Chavez, D.I., Espero, E., Hao, S., Wank, S.A., Raybould, H.E., 2011. Protein hydrolysate-induced cholecystokinin secretion from enteroendocrine cells is indirectly mediated by the intestinal oligopeptide transporter PepT1. Am. J. Physiol. Gastrointest. Liver Physiol. 300 (5), G895–G902. https://doi.org/10.1152/ajpgi.00521.2010.

Liu, Q., Chen, Y., Copeland, D., Ball, H., Duff, R.J., Rockich, B., Londraville, R.L., 2010. Expression of leptin receptor gene in developing and adult zebrafish. Gen. Comp. Endocrinol. 166 (2), 346–355. https://doi.org/10.1016/j.ygcen.2009.11.015.

Liu, Q., Dalman, M., Chen, Y., Akhter, M., Brahmandam, S., Patel, Y., Lowe, J., Thakkar, M., Gregory, A.-V., Phelps, D., Riley, C., Londraville, R.L., 2012. Knockdown of leptin A expression dramatically alters zebrafish development. Gen. Comp. Endocrinol. 178 (3), 562–572. https://doi.org/10.1016/j.ygcen.2012.07.011.

Londraville, R.L., Macotela, Y., Duff, R.J., Easterling, M.R., Liu, Q., Crespi, E.J., 2014. Comparative endocrinology of leptin: assessing function in a phylogenetic context. Gen. Comp. Endocrinol. 203, 146–157. https://doi.org/10.1016/j.ygcen.2014.02.002.

Maffei, M., Halaas, J., Ravussin, E., Pratley, R.E., Lee, G.H., Zhang, Y., Fei, H., Kim, S., Lallone, R., Ranganathan, S., Kern, P.A., Friedman, J.M., 1995. Leptin levels in human and rodent: measurement of plasma leptin and ob RNA in obese and weight-reduced subjects. Nat. Med. 1 (11), 1155–1161. https://doi.org/10.1038/nm1195-1155.

Mania, M., Maruccio, L., Russo, F., Abbate, F., Castaldo, L., D'Angelo, L., de Girolamo, P., Guerrera, M.C., Lucini, C., Madrignano, M., Levanti, M., Germanà, A., 2017. Expression and distribution of leptin and its receptors in the digestive tract of DIO (diet-induced obese) zebrafish. Ann. Anat. 212, 37–47. https://doi.org/10.1016/j.aanat.2017.03.005.

Matsumura, K., Miki, T., Jhomori, T., Gonoi, T., Seino, S., 2005. Possible role of PEPT1 in gastrointestinal hormone secretion. Biochem. Biophys. Res. Commun. 336 (4), 1028–1032. https://doi.org/10.1016/j.bbrc.2005.08.259.

Michel, M., Page-McCaw, P.S., Chen, W., Cone, R.D., 2016. Leptin signaling regulates glucose homeostasis, but not adipostasis, in the zebrafish. Proc. Natl. Acad. Sci. U.S. A. 113 (11), 3084–3089. https://doi.org/10.1073/pnas.1513212113.

Morais, S., 2017. The physiology of taste in fish: potential implications for feeding stimulation and gut chemical sensing. Rev. Fish Sci. Aquac. 25 (2), 133–149. https://doi.org/10.1080/23308249.2016.1249279.

Moschos, S., Chan, J.L., Mantzoros, C.S., 2002. Leptin and reproduction: a review. Fertil. Steril. 77 (3), 433–444. https://doi.org/10.1016/S0015-0282(01)03010-2.

Mun, H.-C., Franks, A.H., Culverston, E.L., Krapcho, K., Nemeth, E.F., Conigrave, A.D., 2004. The Venus Fly Trap domain of the extracellular Ca2+-sensing receptor is required for L-amino acid sensing. J. Biol. Chem. 279 (50), 51739–51744. https://doi.org/10.1074/jbc.M406164/200.

Ohga, H., Matsumori, K., Kodama, R., Kitano, H., Nagano, N., Yamaguchi, A., Matsuyama, M., 2015. Two leptin genes and a leptin receptor gene of female chub mackerel (Scomber japonicus): molecular cloning, tissue distribution and expression in different obesity indices and pubertal stages. Gen. Comp. Endocrinol. 222, 88–98. https://doi.org/10.1016/j.ygcen.2015.06.002.

Ojha, U., 2018. Protein-induced satiation and the calcium-sensing receptor. Diabetes Metab. Syndr. Obes. 11, 45–51. https://doi.org/10.2147/DMSO.S156597.

Opazo, R., Plaza-Parrochia, F., Cardoso Dos Santos, G.R., Carneiro, G.R.A., Sardela, V.F., Romero, J., Valladares, L., 2019. Fasting upregulates *npy*, *agrp*, and *ghsr* without increasing ghrelin levels in zebrafish (*Danio rerio*) larvae. Front. Physiol. 9, 1901. https://doi.org/10.3389/fphys.2018.01901.

Peterson, B.C., Waldbieser, G.C., Riley, L.G., Upton, K.R., Kobayashi, Y., Small, B.C., 2012. Pre- and postprandial changes in orexigenic and anorexigenic factors in channel catfish (Ictalurus punctatus). Gen. Comp. Endocrinol. 176 (2), 231–239. https://doi.org/10.1016/j.ygcen.2012.01.022.

Pelleymounter, M., Cullen, M., Baker, M., Hecht, R., Winters, D., Boone, T., Collins, F., 1995. Effects of the obese gene product on body weight regulation in ob/ob mice. Science 269 (5223), 540–543. https://doi.org/10.1126/science.7624776.

Quinn, S.J., Ye, C.-P., Diaz, R., Kifor, O., Bai, M., Vassilev, P., Brown, E., 1997. The Ca^{2+}-sensing receptor: a target for polyamines. Am. J. Physiol. 273 (4), C1315–C1323. https://doi.org/10.1152/ajpcell.1997.273.4.C1315.

Raybould, H.E., 2007. Mechanisms of CCK signaling from gut to brain. Curr. Opin. Pharmacol. 7 (6), 570–574. https://doi.org/10.1016/j.coph.2007.09.006.

Rombough, P., Drader, H., 2009. Hemoglobin enhances oxygen uptake in larval zebrafish (*Danio rerio*) but only under conditions of extreme hypoxia. J. Exp. Biol. 212, 778–784. https://doi.org/10.1242/jeb.026575.

Rønnestad, I., Rojas-García, C.R., Tonheim, S.K., Conceição, L.E.C., 2001. In vivo studies of digestion and nutrient assimilation in marine fish larvae. Aquaculture 201 (1-2), 161–175. https://doi.org/10.1016/S0044-8486(01)00595-6.

Rønnestad, I., Nilsen, T.O., Murashita, K., Angotzi, A.R., Gamst Moen, A.-G., Stefansson, S.O., Kling, P., Thrandur Björnsson, B., Kurokawa, T., 2010. Leptin and leptin receptor genes in Atlantic salmon: Cloning, phylogeny, tissue distribution and expression correlated to long-term feeding status. Gen. Comp. Endocrinol. 168 (1), 55–70. https://doi.org/10.1016/j.ygcen.2010.04.010.

Rønnestad, I., Akiba, Y., Kaji, I., Kaunitz, J.D., 2014. Duodenal luminal nutrient sensing. Curr. Opin. Pharmacol. 19, 67–75. https://doi.org/10.1016/j.coph.2014.07.010.

Rønnestad, I., Gomes, A.S., Murashita, K., Angotzi, R., Jönsson, E., Volkoff, H., 2017. Appetite-controlling endocrine systems in teleosts. Front. Endocrinol. 8, 73. https://doi.org/10.3389/fendo.2017.00073.

Rosenbaum, M., Nicolson, M., Hirsch, J., Heymsfield, S.B., Gallagher, D., Chu, F., Leibel, R.L., 1996. Effects of gender, body composition, and menopause on plasma concentrations of leptin. J. Clin. Endocrinol. Metab. 81 (9), 3424–3427.

Shutter, J.R., Graham, M., Kinsey, A.C., Scully, S., Luthy, R., Stark, K.L., 1997. Hypothalamic expression of ART, a novel gene related to agouti, is up-regulated in obese and diabetic mutant mice. Genes Dev. 11 (5), 593–602. https://doi.org/10.1101/gad.11.5.593.

Song, Y., Golling, G., Thacker, T.L., Cone, R.D., 2003. Agouti-related protein (AGRP) is conserved and regulated by metabolic state in the zebrafish, Danio rerio. Endocrine 22 (3), 257–266. https://doi.org/10.1385/ENDO:22:310.1385/ENDO:22:3:257.

Stanley, B.G., Leibowitz, S.F., 1985. Neuropeptide Y injected in the paraventricular hypothalamus: a powerful stimulant of feeding behavior. Proc. Natl. Acad. Sci. U.S. A. 82 (11), 3940–3943. https://doi.org/10.1073/pnas.82.11.3940.

Tang, L., Cheng, C.Y., Sun, X., Pedicone, A.J., Mohamadzadeh, M., Cheng, S.X., 2016. The extracellular calcium-sensing receptor in the intestine: evidence for regulation of colonic absorption, secretion, motility, and immunity. Front. Physiol. 7, 245. https://doi.org/10.3389/fphys.2016.00245.

Tuttle, M., Dalman, M.R., Liu, Q., Londraville, R.L., 2019 Leptin-a mediates transcription of genes that participate in central endocrine and phosphatidylinositol signaling pathways in 72-hour embryonic zebrafish (Danio rerio). PeerJ. 7, e6848. https://doi.org/10.7717/peerj.6848.

Uniappan, S., Kieffer, T.J., 2008. Leptin extends the anorectic effect chronic PYY (3-36) administration in ad libitum-fed rats. Am. J. Physiol. Integr. Comp. Physiol. 295, R51-R58. https://doi.org/10.1152/ajpregu.00234.2007.

Vacca, F., Barca, A., Gomes, A.S., Mazzei, A., Piccinni, B., Cinquetti, R., Del Vecchio, G., Romano, A., Rønnestad, I., Bossi, E., Verri, T., 2019. The peptide transporter 1a of the zebrafish *Danio rerio*, an emerging model in nutrigenomics and nutrition research: molecular characterization, functional properties, and expression analysis. Genes Nutr. 14, 33. https://doi.org/10.1186/s12263-019-0657-3.

Valen, R., Jordal, A.-E.-O., Murashita, K., Rønnestad, I., 2011. Postprandial effects on appetite-related neuropeptide expression in the brain of Atlantic salmon, *Salmo salar*. Gen. Comp. Endocrinol. 171 (3), 359–366. https://doi.org/10.1016/j.ygcen.2011.02.027.

Verri, T., Kottra, G., Romano, A., Tiso, N., Peric, M., Maffia, M., Boll, M., Argenton, F., Daniel, H., Storelli, C., 2003. Molecular and functional characterization of the zebrafish (Danio rerio) PEPT1-type peptide transporter. FEBS Lett. 549, 115–122. https://doi.org/10.1016/s0014-5793(03)00759-2.

Volkoff, H., Eykelbosh, A.J., Peter, R.E., 2003. Role of leptin in the control of feeding of goldfish *Carassius auratus*: interactions with cholecystokinin, neuropeptide Y and orexin A, and modulation by fasting. Brain Res. 972, 90–109. https://doi.org/10.1016/s0006-8993(03)02507-1.

Volkoff, H., Peter, R.E., 2001. Characterization of two forms of cocaine- and amphetamine-regulated transcript (CART) peptide precursors in goldfish: molecular cloning and distribution, modulation of expression by nutritional status, and interactions with leptin. Endocrinology 142, 5076–5088. https://doi.org/10.1210/endo.142.12.8519.

Volkoff, H., Canosa, L.F., Unniappan, S., Cerdá-Reverter, J.M., Bernier, N.J., Kelly, S.P., Peter, R.E., 2005. Neuropeptides and the control of food intake in fish. Gen. Comp. Endocrinol. 142 (1-2), 3–19. https://doi.org/10.1016/j.ygcen.2004.11.001.

Volkoff, H., 2016. The neuroendocrine regulation of food intake in fish: a review of current knowledge. Front. Neurosci. 10, 540. https://doi.org/10.3389/fnins.2016.00540.

Wallace, K.N., Pack, M., 2003. Unique and conserved aspects of gut development in zebrafish. Dev. Biol. 255 (1), 12–29. https://doi.org/10.1016/S0012-1606(02)00034-9.

Wallace, K.N., Akhter, S., Smith, E.M., Lorent, K., Pack, M., 2005. Intestinal growth and differentiation in zebrafish. Mech. Dev. 122 (2), 157–173. https://doi.org/10.1016/j.mod.2004.10.009.

Wang, M., Yao, Y.i., Kuang, D., Hampson, D.R., 2006. Activation of family C G-protein-coupled receptors by the tripeptide glutathione. J. Biol. Chem. 281 (13), 8864–8870. https://doi.org/10.1074/jbc.M512865200.

Wilson, B.D., Bagnol, D., Kaelin, C.B., Ollmann, M.M., Gantz, I., Watson, S.J., Barsh, G.S., 1999. Physiological and anatomical circuitry between agouti-related protein and leptin signaling. Endocrinology 140, 2387–2397. https://doi.org/10.1210/endo.140.5.6728.

Yan, A.F., Chen, T., Chen, S., Ren, C.H., Hu, C.Q., Cai, Y.M., Liu, F., Tang, D.S., 2016. Goldfish leptin-AI and leptin-AII: Function and central mechanism in feeding control. Int. J. Mol. Sci. 17, 783–796. https://doi.org/10.3390/ijms17060783.

Yang, Q., Yan, C., Wang, X., Gong, Z., 2019. Leptin induces muscle wasting in a zebrafish *kras*-driven hepatocellular carcinoma (HCC) model. Dis. Model. Mech. 12, dmm038240. https://doi.org/10.1242/dmm.038240.

Yarandi, S.S., Hebbar, G., Sauer, C.G., Cole, C.R., Ziegler, T.R., 2011. Diverse roles of leptin in the gastrointestinal tract: modulation of motility, absorption, growth, and inflammation. Nutrition 27 (3), 269–275. https://doi.org/10.1016/j.nut.2010.07.004.

Yokobori, E., Azuma, M., Nishiguchi, R., Kang, K.S., Kamijo, M., Uchiyama, M., Matsuda, K., 2012. Neuropeptide Y stimulates food intake in the zebrafish, Danio rerio. J. Neuroendocrinol. 24, 766–773. https://doi.org/10.1111/j.1365-2826.2012.02281.x.

Yuan, X., Li, A., Liang, X.F., Huang, W., Song, Y., He, S., Cai, W., Tao, Y.X., 2016. Leptin expression in mandarin fish Siniperca chuatsi (Basilewsky): regulation by postprandial and short-term fasting treatment. Comp. Biochem. Physiol. A Mol. Integr. Physiol. 194, 8–18. https://doi.org/10.1016/j.cbpa.2016.01.014.

Yuan C, X, Liang F, X, Cai J, W, He, S, Guo J, W, Mai S, K, 2020. Expansion of sweet taste receptor genes in grass carp (*Ctenopharyngodon idellus*) coincided with vegetarian adaptation. BMC Evol. Biol. 20, 25. https://doi.org/10.1186/s12862-020-1590-1.

Zhang, L., Nguyen, A.D., Lee, I.C.J., Yulyaningsih, E., Riepler, S.J., Stehrer, B., Enriquez, R.F., Lin, S., Shi, Y.C., Baldock, P.A., Sainsbry, A., Herzog, H., 2012. NPY modulates PYY function in the regulation of energy balance and glucose homeostasis. Diabetes Obes. Metab. 14, 727–736. https://doi.org/10.1111/j.1463-1326.2012.01592.x.

Zhang, Y.Y., Chua, S., 2018. Leptin function and regulation. Compr. Physiol. 8, 351–369. https://doi.org/10.1002/cphy.c160041.

Zieba, D.A., Amstalden, M., Williams, G.L., 2005. Regulatory roles of leptin in reproduction and metabolism: a comparative review. Domest. Anim. Endocrinol. 29 (1), 166–185. https://doi.org/10.1016/j.domaniend.2005.02.019.